nature medicine

Article

https://doi.org/10.1038/s41591-023-02645-5

# Prevalence of chromosomal alterations in first-trimester spontaneous pregnancy loss

Received: 26 May 2023

Accepted: 11 October 2023

Published online: 23 November 2023

Check for updates

Rick Essers[1,2,16], Igor N. Lebedev[3,16], Ants Kurg[4,16], Elizaveta A. Fonova[3], Servi J. C. Stevens[1,2], Rebekka M. Koeck[1,2], Ulrike von Rango[5], Lloyd Brandts[6], Spyridon Panagiotis Deligiannis[7,8], Tatyana V. Nikitina[3], Elena A. Sazhenova[3], Ekaterina N. Tolmacheva[3], Anna A. Kashevarova[3], Dmitry A. Fedotov[3], Viktoria V. Demeneva[3], Daria I. Zhigalina[3], Gleb V. Drozdov[3], Salwan Al-Nasiry[2,9], Merryn V. E. Macville[1,2], Arthur van den Wijngaard[1,2], Jos Dreesen[1], Aimee Paulussen[1,2], Alexander Hoischen[10,11,12,13], Han G. Brunner[1,2,10], Andres Salumets[7,14,15,17] ✉ & Masoud Zamani Esteki[1,2,15,17] ✉

Pregnancy loss is often caused by chromosomal abnormalities of the conceptus. The prevalence of these abnormalities and the allocation of (ab)normal cells in embryonic and placental lineages during intrauterine development remain elusive. In this study, we analyzed 1,745 spontaneous pregnancy losses and found that roughly half (50.4%) of the products of conception (POCs) were karyotypically abnormal, with maternal and paternal age independently contributing to the increased genomic aberration rate. We applied genome haplarithmisis to a subset of 94 pregnancy losses with normal parental and POC karyotypes. Genotyping of parental DNA as well as POC extra-embryonic mesoderm and chorionic villi DNA, representing embryonic and trophoblastic tissues, enabled characterization of the genomic landscape of both lineages. Of these pregnancy losses, 35.1% had chromosomal aberrations not previously detected by karyotyping, increasing the rate of aberrations of pregnancy losses to 67.8% by extrapolation. In contrast to viable pregnancies where mosaic chromosomal abnormalities are often restricted to chorionic villi, such as confined placental mosaicism, we found a higher degree of mosaic chromosomal imbalances in extra-embryonic mesoderm rather than chorionic villi. Our results stress the importance of scrutinizing the full allelic architecture of genomic abnormalities in pregnancy loss to improve clinical management and basic research of this devastating condition.

Worldwide, 23 million pregnancy losses occur every year, with a high prevalence of 10–15% of all clinically recognized pregnancies[1]. Pregnancy loss primarily occurs before weeks 8–9 of gestation[1], and there is considerable additional loss in earlier stages of pregnancy that may go unnoticed. Overall, 10.8% of women experience at least one pregnancy loss, and 1.9% and 0.7% have two or three pregnancy losses, respectively[1]. Identifying the cause of pregnancy loss can provide important prognostic, diagnostic and management recommendations to support future viable pregnancies[2]. Chromosomal abnormalities, in particular aneuploidy, defined as an incorrect number of chromosomes,

A full list of affiliations appears at the end of the paper. ✉e-mail: andres.salumets@ki.se; masoud.zamaniesteki@mumc.nl

https://doi.org/10.1038/s41591-023-02645-5

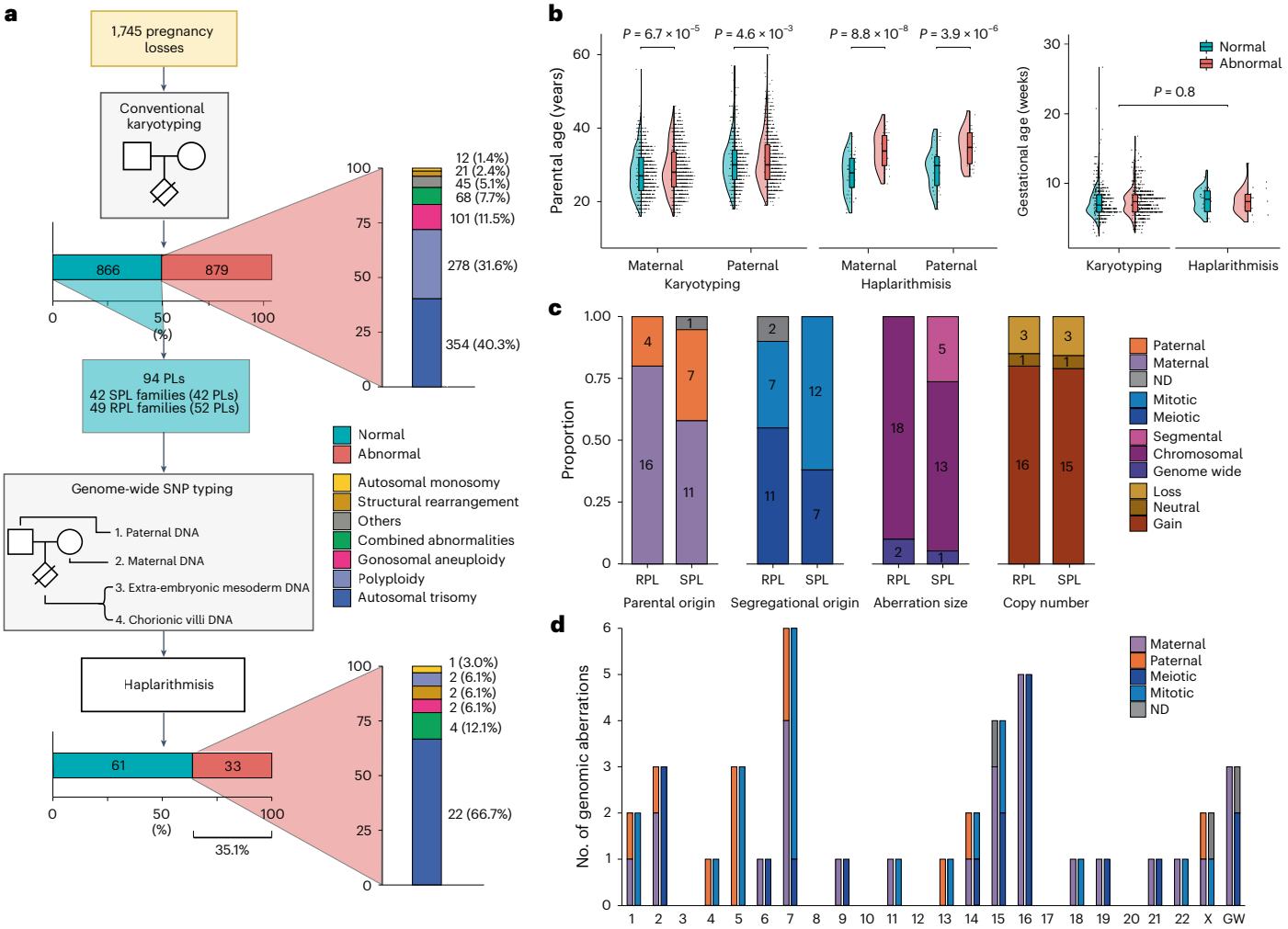


**Fig. 1 | Genome haplarithmisis reveals previously undetected chromosomal aberrations. a**, Study design and distribution of aberrations. **b**, Maternal, paternal and gestational age in conventional karyotyping of POC samples with normal ($n = 866$) and abnormal ($n = 879$) karyotypes and in genome haplarithmisis POC samples with normal ($n = 61$) and abnormal ($n = 33$) genomes (two-sided Welch's $t$-test). The box plot represents the 25th percentile, median and 75th percentile, respectively, and the whiskers extend to the farthest data point that is no more than 1.5 times the interquartile range (IQR) from the upper or lower quartile. **c**, Parental and segregational origin of aberrations, aberration size (segmental, chromosomal and genome wide) and copy number (gain, loss and neutral) of unique aberrations per POC sample for the RPL cohort ($n = 20$) and the SPL cohort ($n = 19$). **d**, Parental and segregational origin of genomic aberration per chromosome, including each unique aberration per POC sample. PL, pregnancy loss. ND, not determined; POC, product of conception; SPL, sporadic pregnancy loss; RPL, recurrent pregnancy loss.

in the conceptus are the leading causes of pregnancy losses. It has been established that aneuploidies commonly occur during oogenesis[3–5] and in early embryogenesis[6–8]. The incidence of chromosomal aneuploidies increases with maternal age, which contributes to age-related infertility[8]. This is due to the low fidelity of chromosome segregation in meiosis during oogenesis[3,8] and DNA replication stress[9] during mitotic cleavage divisions in pre-implantation embryogenesis[6,7]. Previously, we and others demonstrated that, although chromosome instability (CIN) is common in early embryogenesis[6,7], it is not present at birth[10]. This observation indicates that only embryos with sufficient genome integrity can survive to term and that both meiotic aneuploidies in oocytes and post-zygotic chromosome abnormalities in early embryogenesis may lead to implantation failure and pregnancy losses[1].

CIN leads to mosaic embryos that contain both chromosomally normal and abnormal cells. It has been shown that aneuploid cells in mosaic embryos can be progressively depleted during pre-implantation development[11]. Self-correction of human embryos may operate via cellular fragmentation and blastomere exclusion of abnormal cells[12] or by rescue mechanisms, such as trisomy or monosomy rescue[13]. Spatiotemporal allocation of abnormal cells or aneuploidy rescue mechanisms can lead to confined placental mosaicism, which is the main biological cause for discordant abnormal non-invasive prenatal

**Table 1 | Clinical diagnosis of early pregnancy loss**

| Diagnosis | Conventional karyotyping | | Genome haplarithmisis | |
|---|---|---|---|---|
| | *n* | % | *n* | % |
| Missed abortions | 1,156 | 66.2 | 74 | 78.7 |
| Anembryonic pregnancies | 261 | 15.0 | 16 | 17.0 |
| Spontaneous abortions | 137 | 7.9 | 1 | 1.1 |
| Fetus malformations | 27 | 1.5 | 0 | 0 |
| Hydatidiform mole | 4 | 0.2 | 0 | 0 |
| Inconclusive pregnancy loss etiology | 160 | 9.2 | 3 | 3.2 |
| Total POCs | 1,745 | 100 | 94 | 100 |

testing (NIPT) results, with normal fetus confirmed after invasive fetal testing[14]. For instance, we previously showed that more than 70% of large (>100 kilobase (kb)) de novo copy number variations (CNVs) are present only in the placental lineage[10].

The genomic landscape of second-trimester and third-trimester pregnancy losses and elective terminations of fetuses with abnormal in utero phenotypes has been characterized[15]. However, little is known about the genomic landscape of first-trimester spontaneous pregnancy losses. This knowledge is essential to understanding in utero mechanisms of CIN separately for fetal and placental lineages and to developing strategies for the early detection of high-risk pregnancies leading to pregnancy loss. In this study, we profiled the chromosomal landscape of the chorionic villi and the extra-embryonic mesoderm of first-trimester (~7 weeks of gestational age) spontaneous pregnancy losses, which are derived from the embryonic trophectoderm and the inner cell mass, respectively.

## Results

### Cohort characteristics and conventional cytogenetic tests

After conventional karyotyping of the products of conception (POCs) that were collected from 1,745 women over a course of 35 years (1987–2021), 866 (49.6%) and 879 (50.4%) pregnancy losses were classified as karyotypically normal and abnormal, respectively (Fig. 1a and Table 1). Of the 1,745 cases, 1,597 (91.5%) samples were karyotyped using conventional GTG banding after long-term extra-embryonic fibroblast culture, and 29 (1.7%) samples were karyotyped by direct preparations of the chorionic villi. If GTG banding was not possible, other traditional methods, including conventional comparative genomic hybridization (CGH) (3.4%, 59 samples) and interphase fluorescence in situ hybridization (FISH) with centromere enumeration probes (3.4%, 60 samples), were performed.

In line with previous studies[1,16,17], abnormal fetal karyotypes were associated with higher parental age (maternal age: 29.0 ± 6.4 s.d. and 27.8 ± 5.9 s.d., respectively, $P = 6.7 \times 10^{-5}$; paternal age: 31.3 ± 6.8 s.d. and 30.3 ± 6.3 s.d., respectively, $P = 4.6 \times 10^{-3}$; two-sided Welch's *t*-test) (Fig. 1b). Logistic regression was performed to further investigate whether maternal and paternal age were independently associated with abnormal POC karyotypes. Implementing both parental ages in the same regression model dissolved the statistically significant association for both factors, indicating that maternal and paternal age separately explain the same variance in the data and show high collinearity (Supplementary Table 1).

### Genomic alterations in karyotypically normal POCs

We analyzed 94 karyotypically normal pregnancy losses with good-quality DNA samples (Methods) from 91 families with similar gestational ages as the entire cohort (7.5 ± 2.2 s.d. and 7.5 ± 1.7 s.d. gestational weeks, respectively, $P = 0.8$, two-sided Welch's *t*-test) (Fig. 1b and Methods). These samples were selected based on (1) their classification as 'normal' by conventional karyotyping; (2) the availability of POC extra-embryonic mesoderm and chorionic villi tissues and parental DNA; and (3) parents who were were karyotypically normal, without genetic predisposition for pregnancy loss. To detect (mosaic) de novo genomic aberrations in POCs undetected by conventional karyotyping, we performed genome-wide single-nucleotide polymorphism (SNP) genotyping of parental as well as extra-embryonic mesoderm and chorionic villi DNA from POCs, followed by genome haplarithmisis[7,10]. Haplarithmisis is a conceptual method that transforms genotyping data to haplotypes and copy number states, called parental haplarithms. When a copy number change affects a combination of different homologous chromosomes of a parent, this represents meiotic error. If the centromere is from different homologous chromosomes, this represents meiotic I error. If the centromere is not involved, but a part of the chromosome derives from different homologous chromosomes, this specifies meiotic II error[18]. In addition, distortion of B-allele frequency (BAF) values from expected $1_{maternal}$:$1_{paternal}$ allelic ratio indicates the degree (%) of abnormal cells—that is, mosaicism[10,19]. Here, we applied haplarithmisis on bulk DNA samples (that is, derived from many cells) and made use of chorionic villi as a seed to phase the parental genomes, allowing the reconstruction of trio-based parental haplarithms (Fig. 2a and Methods). This allowed us to determine the prevalence and nature of different chromosomal abnormalities, including their parental and mechanistic origins (Figs. 1c,d and 2a,b) and their levels of mosaicism (Fig. 2a,b and Extended Data Fig. 1). The data showed that, of 94 POCs (188 paired chorionic villi and extra-embryonic mesoderm DNA samples; 89 families with a single pregnancy loss, one family with two pregnancy losses and one family with three pregnancy losses), 65 DNA samples (34.6%; 33 chorionic villi and 32 extra-embryonic mesoderm DNA samples) had a genomic aberration (Source Data). Thus, out of 94 karyotypically normal POC samples, as determined by conventional analysis, 33 POC samples (35.1%) had one or more genomic imbalances that were detected by genome haplarithmisis (Fig. 1a and Supplementary Table 2). If we consider these haplarithmisis-determined abnormal samples (35.1%) as well as the 50.4% abnormality rate reported through conventional karyotyping ($n = 879/1,745$), the rate of genomic aberrations in POC samples reaches 67.8% by extrapolation (Methods). This is higher than what has been quoted previously by other studies that used karyotyping[13,20] or clinical-grade chromosomal microarrays[21–29] (Supplementary Table 3).

### Profiling the genomic landscape of sporadic and recurrent pregnancy losses

To further characterize the genetic effect of the detected aberrations, we divided the 94 pregnancy losses into sporadic pregnancy loss (SPL), defined as one pregnancy loss (42 families and pregnancy losses, 84 DNA samples), and recurrent pregnancy loss (RPL), defined as two or more consecutive pregnancy losses (49 families, 52 pregnancy losses, 104 DNA samples) (Fig. 1a). The SPL and RPL cohorts had 28 (33.3%, 19 unique copy number aberrations per POC) and 37 (35.6%, 20 unique copy number aberrations per POC) POC samples with genomic aberrations, respectively (Extended Data Fig. 2). The RPL and SPL cohorts did not show a significant difference in either segregational and parental origins of aberrations or in the total copy number or copy-neutral events (Fig. 1c). However, the SPL cohort contained more segmental aberrations, whereas the RPL cohort contained more numerical chromosomal aberrations (Fig. 1c; $P = 3.6 \times 10^{-2}$, Fisher's exact test).

Aberrations on Chr 7 and Chr 16 were most common in first-trimester pregnancy loss (Fig. 1d), as observed previously[1,30]. Aberrations on Chr 16 ($n = 5$) were all of maternal and meiotic in origin,

**Fig. 2 | Schematic representation of genome haplarithmisis and detection of various abnormalities. a**, A genomic region harboring three consecutive SNPs, each with weighted signal intensity of 10, as well as equation for BAF computation for those three SNPs. **b**, Schematic representation of the standard genome haplarithmisis workflow as demonstrated in Zamani Esteki et al.[7]. Detection of different levels of mosaicism in trio-based haplarithmisis (**c**) and parental and segregational origin of genomic anomalies in trio-based haplarithmisis (**d**) (Methods). **e**, Haplarithms of several pregnancy losses with different types of abnormalities, parental and segregational origins and mosaicism degrees; only a single chromosome of interest is displayed per POC sample. PL1063 has a normal diploid Chr 3; PL1595 has a non-mosaic trisomy 18 of maternal and mitotic error origin; PL140 has a non-mosaic trisomy 16 of maternal and meiosis I error origin; PL1783 has a non-mosaic trisomy 2 of paternal and meiosis II error origin; PL1701 has an approximately 40% mosaic trisomy 5 of paternal and mitotic error origin; PL2074 has an approximately 50% mosaic monosomy 7 of paternal (maternal chromosome is left) and mitotic error origin; PL1618 has a (subchromosomal) approximately 2.7-Mb duplication in Chr 5 near the centromere (q11.1–q11.2) of paternal and mitotic error origin; PL2726 has an approximately 65% mosaic UPD 1 of maternal and mitotic origin; and PL1758 has a tetrasomy 7 of maternal error origin (Extended Data Fig. 7). PL, pregnancy loss.

https://doi.org/10.1038/s41591-023-02645-5

and aberrations on Chr 7 were maternal and mitotic ($n = 4$), paternal and mitotic ($n = 1$) and paternal and meiotic ($n = 1$) in origin (Fig. 1d). Trisomy 16 impairs embryonic growth due to placental hyperplasia, potentially leading to first-trimester pregnancy loss[30]. Trisomy 16 is less prevalent in NIPT samples at 11–12 weeks of pregnancy[31,32] as compared to pre-implantation embryos after pre-implantation genetic testing (PGT)[33,34], indicating that pregnancies with trisomy 16 may have reduced capacity to reach to later gestational ages.

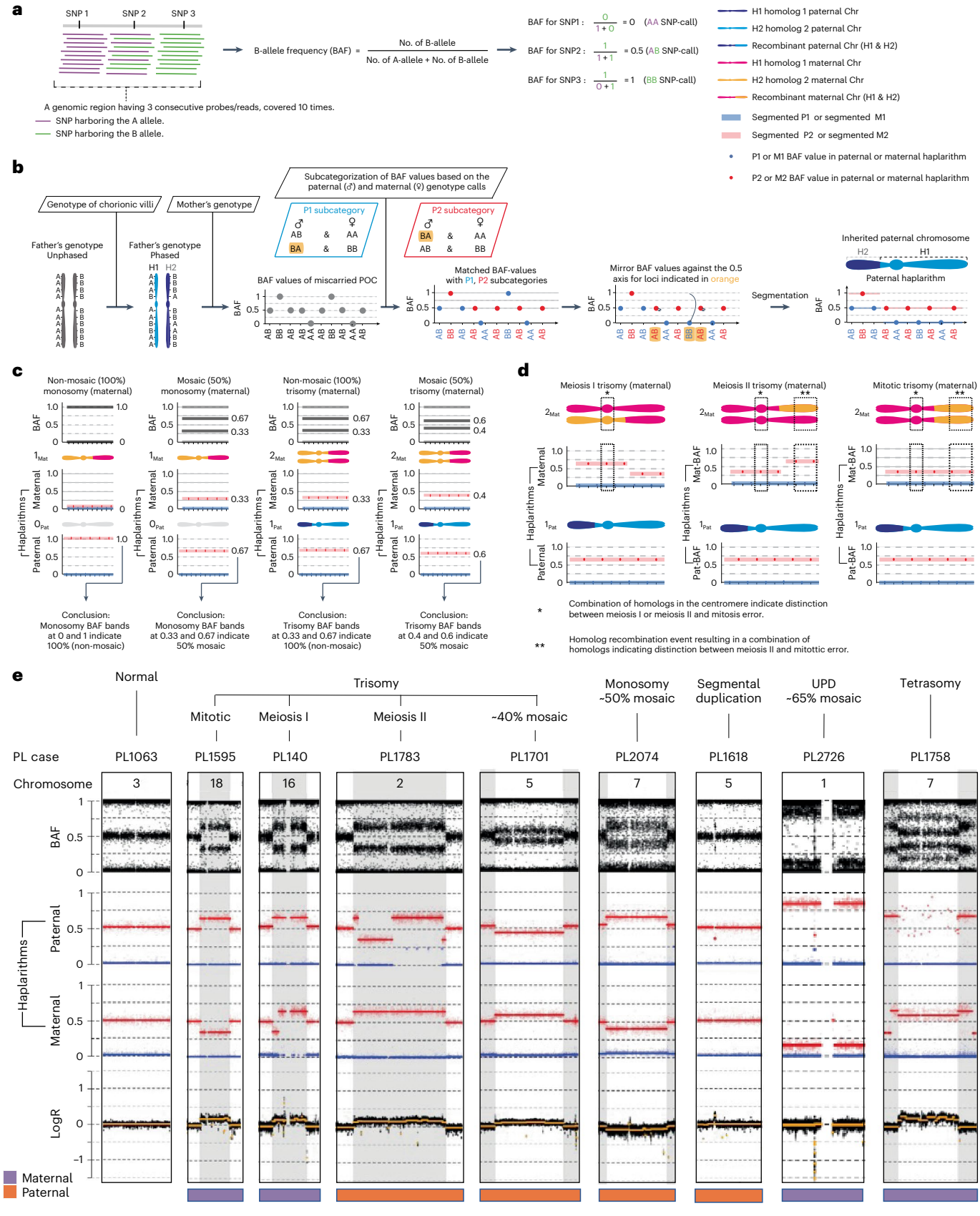

https://doi.org/10.1038/s41591-023-02645-5

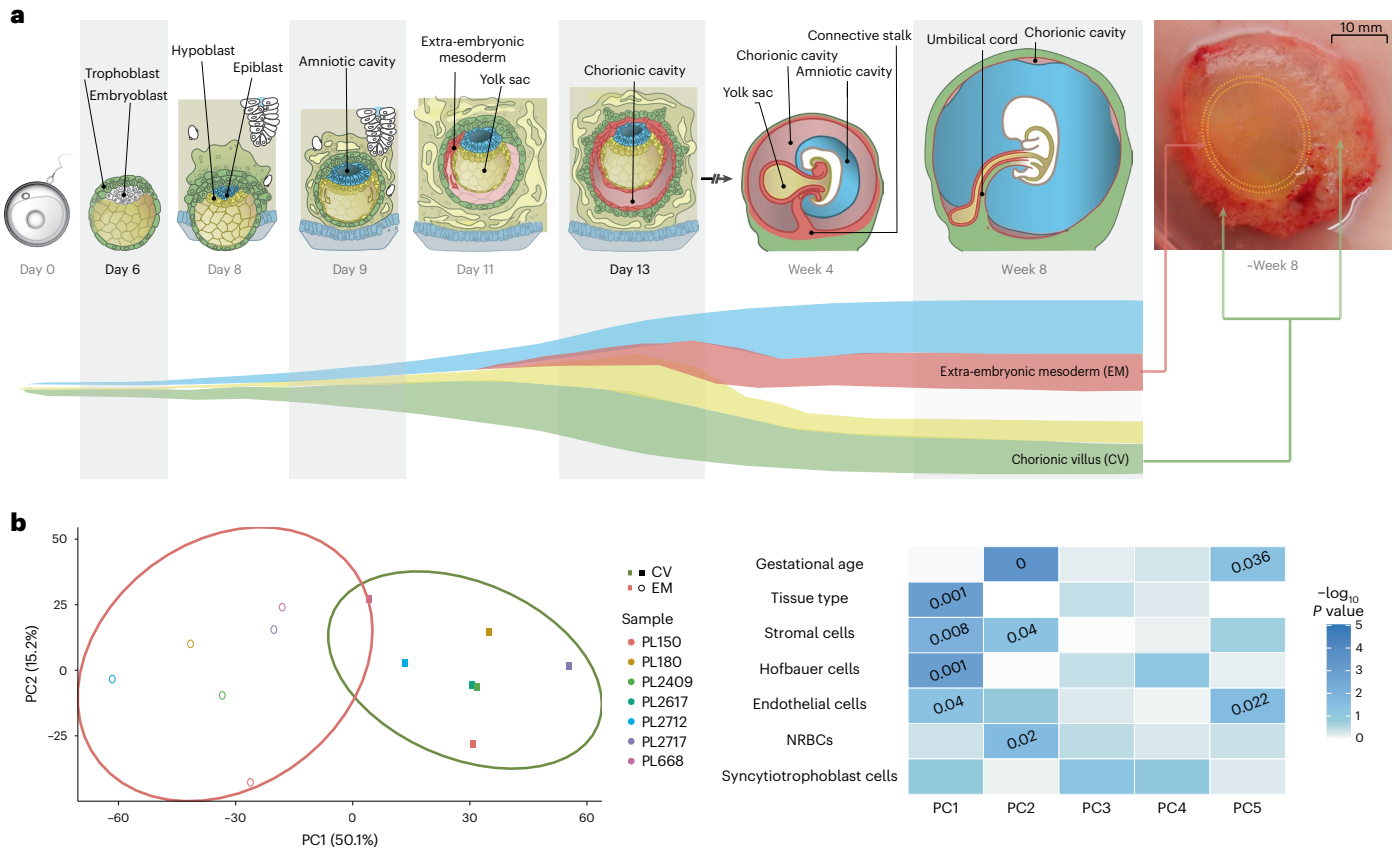


**Fig. 3 | Extra-embryonic mesoderm and chorionic villi lineages and their cellular composition. a**, Schematic representation of early embryonic development. Extra-embryonic mesoderm (EM) develops from the embryoblast lineage (hypoblast and epiblast), whereas chorionic villi (CV) develop from the trophoblast lineage. EM and CV samples from pregnancy losses were collected at week 7.6 ± 1.7 s.d. **b**, PCA of all CpG sites ($n$ = 685,221) passing quality control criteria (Methods) in data from high-DNA-quality EM ($n$ = 6) and CV ($n$ = 7) samples. The ellipses represent the 90% confidence interval, and the percentage of variance explained by each principal component (PC) is shown in brackets. Heat map showing associations between the first five PCs and biological aspects of the samples, including their predicted cell compositions (Extended Data Fig. 6). The color gradient shows the $-\log_{10}$ of the $P$ values, and $P$ values less than 0.05 are indicated. The significance of the correlation between the PCs and the continuous, numerical sample attributes was tested using a permutation test with 10,000 permutations. The association between the PCs and the binary variable tissue type was assessed using a two-sided Wilcoxon signed-rank test.

## Determining the level of mosaicism in chorionic villi and extra-embryonic mesoderm tissues

Comparing the haplarithm profiles of extra-embryonic mesoderm and chorionic villi allowed us to determine not only if these tissues carry different large CNVs (>100 kb) but also whether the level of mosaicism is different. The analysis of extra-embryonic mesoderm and chorionic villi DNA samples can be used to probe the spatiotemporal allocation of abnormal cells in early embryogenesis and to deduce whether this allocation affects the fate of early prenatal development and the risk of pregnancy loss. To check for accurate dissection of extra-embryonic mesoderm and chorionic villi tissues, we performed methylome-wide analysis of 13 samples that generated good-quality data (Extended Data Fig. 3 and Methods). Principal component analysis (PCA) of all methylation sites showed clear separation of chorionic villi and extra-embryonic mesoderm tissues (Fig. 3b). Subsequent cell composition deconvolution suggested that both chorionic villi and extra-embryonic mesoderm samples were of mixed, but different, cellular origin, with a significantly higher proportion of Hofbauer cells as well as a significantly lower proportion of stromal cells in chorionic villi samples compared to the extra-embryonic mesoderm samples (Extended Data Fig. 4).

Although there is no doubt that the chorionic villi are derived from the trophectoderm[35,36], there is some uncertainty surrounding the developmental origin of extra-embryonic mesoderm[35,36]. A recent study proposed that the extra-embryonic mesoderm develops from the hypoblast-derived primary yolk sac, supplemented by epiblast-derived mesoderm from the gastrulating embryo[35] (Fig. 3a and Extended Data Fig. 5). Hypoblasts and epiblasts are both derived from the inner cell mass. Of the 33 genetically aberrant POC samples, a selection consisting of all tissues with a mitotic aberration or meiotic aberration with a greater than 10% difference in the proportion of abnormal cells comparing extra-embryonic mesoderm and chorionic villi showed that the extra-embryonic mesoderm biopsies had a higher level of mosaicism relative to chorionic villi (58.2% ± 30.1 s.d. and 43.4% ± 32.9 s.d., respectively, $P = 2.0 \times 10^{-2}$, Wilcoxon signed-rank test; Fig. 4). Of the nine POC samples (27.3%) with a greater than 10% difference in level of mosaicism, eight samples (six aberrations of mitotic origin and two of meiotic origin) had aberrations in autosomes and one sample (aberration of mitotic origin) in Chr X (Fig. 5). In all samples with autosomal aberrations, the level of mosaicism was higher in extra-embryonic mesoderm than in chorionic villi (Figs. 4 and 5). This contrasts with viable pregnancies where mosaic abnormalities are often restricted to the chorionic villi[35,36]. For two cases, copy number aberrations (trisomy 13 of PL2726 and monosomy 7 of PL2074; Fig. 5 and Extended Data Fig. 5) were detected only in extra-embryonic mesoderm, with post-zygotic mitotic origin. These support the theoretical model for tissue-specific aneuploid cell line compartmentalization in early pregnancy loss[13].

https://doi.org/10.1038/s41591-023-02645-5

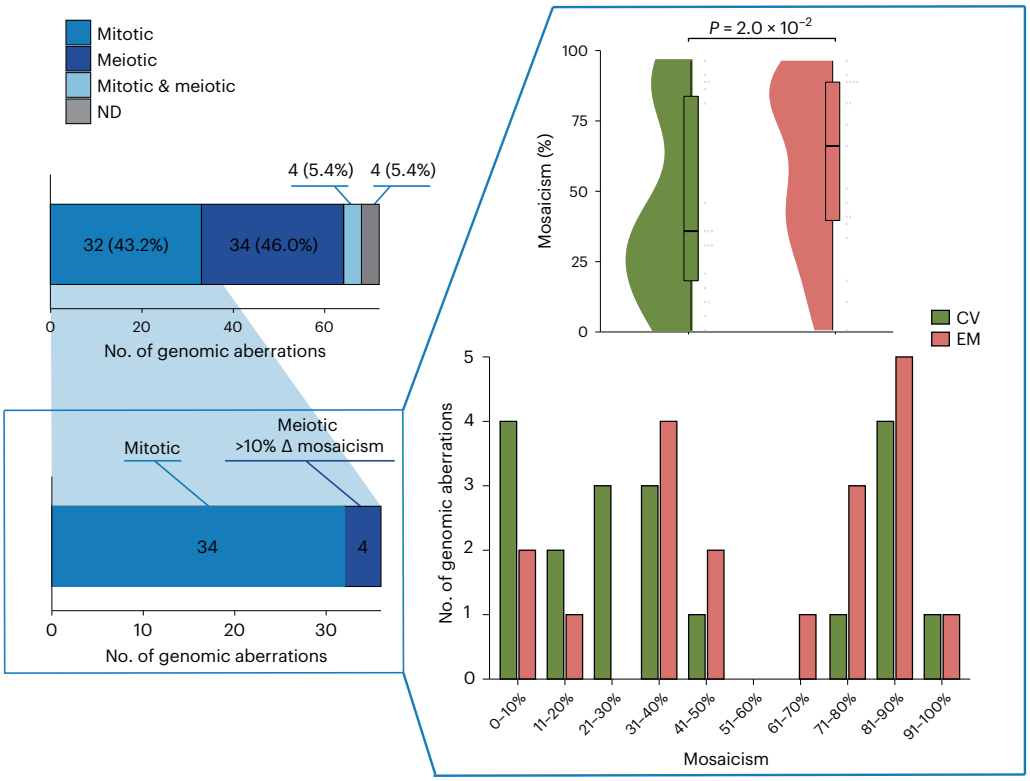


**Fig. 4 | Segregational and lineage origins of pregnancy losses.** Segregational origin of each individual aberration in both extra-embryonic mesoderm (EM) and chorionic villi (CV) tissue per POC detected by genome haplarithmisis, whereas samples with aberrations of mitotic origin ($n = 34$: 17 EM and 17 CV) or meiotic origin with greater than 10% mosaicism difference between EM and CV ($n = 4$: two EM and two CV) were selected for EM/CV plots and mosaicism statistics. The mosaicism degree in EM samples ($n = 19$) was significantly higher than that in CV samples ($n = 19$) (two-sided Wilcoxon signed-rank test). The box plot represents the 25th percentile, median and 75th percentile, respectively, whereas the whiskers extend to the farthest data point that is no more than 1.5 times the interquartile range (IQR) from the upper or lower quartile. ND, not determined.

## Discussion

Even though CIN is common in early embryogenesis and leads to mosaic embryos carrying both chromosomally normal and abnormal cells[6,7], the abnormal cells are not predominantly present at birth[10]. However, the effect of post-zygotic CIN on first-trimester prenatal development is not clear. In this study, we carried out parallel analysis of extra-embryonic mesoderm and chorionic villi samples from the same POCs, increasing the diagnostic yield of detecting genomic aberrations. Strikingly, mosaicism tended to be higher in extra-embryonic mesoderm relative to chorionic villi, which again suggests persistent involvement of abnormal fetal cells in pregnancy loss. Over 90% of pregnancy losses occur during the first trimester[37,38]. Chromosomal abnormalities in the fetus are recognized as a primary cause of pregnancy loss. Previously, eight large studies (>1,000 POC sample size, in total 42,500 POCs) showed a combined yield of approximately 53.7% fetal chromosomal abnormalities[21–28] (Supplementary Table 3), which is in line with the 53.1% reported rate in a recent meta-analysis[29]. The study that applied high-density SNP arrays reported a higher yield of 67%, which is similar to what we found here, in the present study, after genome haplarithmisis[26]. Thus, haplarithmisis gives a superior yield over karyotyping or standard microarray approach. In addition, six previous studies analyzed POCs that were classified as normal with conventional karyotyping[39–44] (Supplementary Table 4). The average frequency of additionally detected abnormalities found in these studies was 19.4%, which is nearly two-fold lower than the 35.1% identified in the present study. This difference can be explained by two major factors. First, the previous studies relied on single POC tissue analysis, primarily chorionic villi or placenta. Second, the conventional cytogenetic methods, including microarrays, are unable to distinguish the meiotic and mitotic origins of genomic aberrations and detect low-level mosaicism. Here we demonstrate that these shortcomings can be tackled using genome haplarithmisis.

The conventional karyotyping of POCs being applied in routine care is limited by its low resolution, contamination from maternal cells, high culture failure rates and overgrowth of (maternal) normal cells compared to abnormal cells, leading to low diagnostic yield[45]. The quality also varies between samples and laboratories and is reliant on the expertise of technicians and cytogeneticists. Previously, we and others showed that low proliferative activity of extra-embryonic cells in vitro is a major limitation of conventional karyotyping of spontaneous pregnancy losses. Specifically, conventional cytogenetic analysis of miscarriages strongly depends on tissue culturing and is associated with a substantial culture failure rate, which varies from 5% to 42% in different laboratories[46–55]. This suggests that the use of sophisticated genome analysis methods that use DNA samples and do not require cell culturing in pregnancy loss samples carry clear advantages. Genome haplarithmisis can detect low-grade mosaicism (>10%) from uncultured samples (Fig. 2a, Extended Data Fig. 1 and Methods) with higher resolution and allows for the detection of smaller subchromosomal CNVs (>100 kb) (Fig. 2e and Extended Data Fig. 1b)[10]. Additionally, it can detect the parental and segregational origins of aberrations and maternal cell contamination[7] (Fig. 2d and Extended Data Figs. 6 and 7). These features are well beyond the sensitivity of conventional methods, such as karyotyping and standard chromosomal microarray-based or sequencing-based copy number analyses that are being performed in routine care. There is an emerging need for prospective clinical studies

https://doi.org/10.1038/s41591-023-02645-5

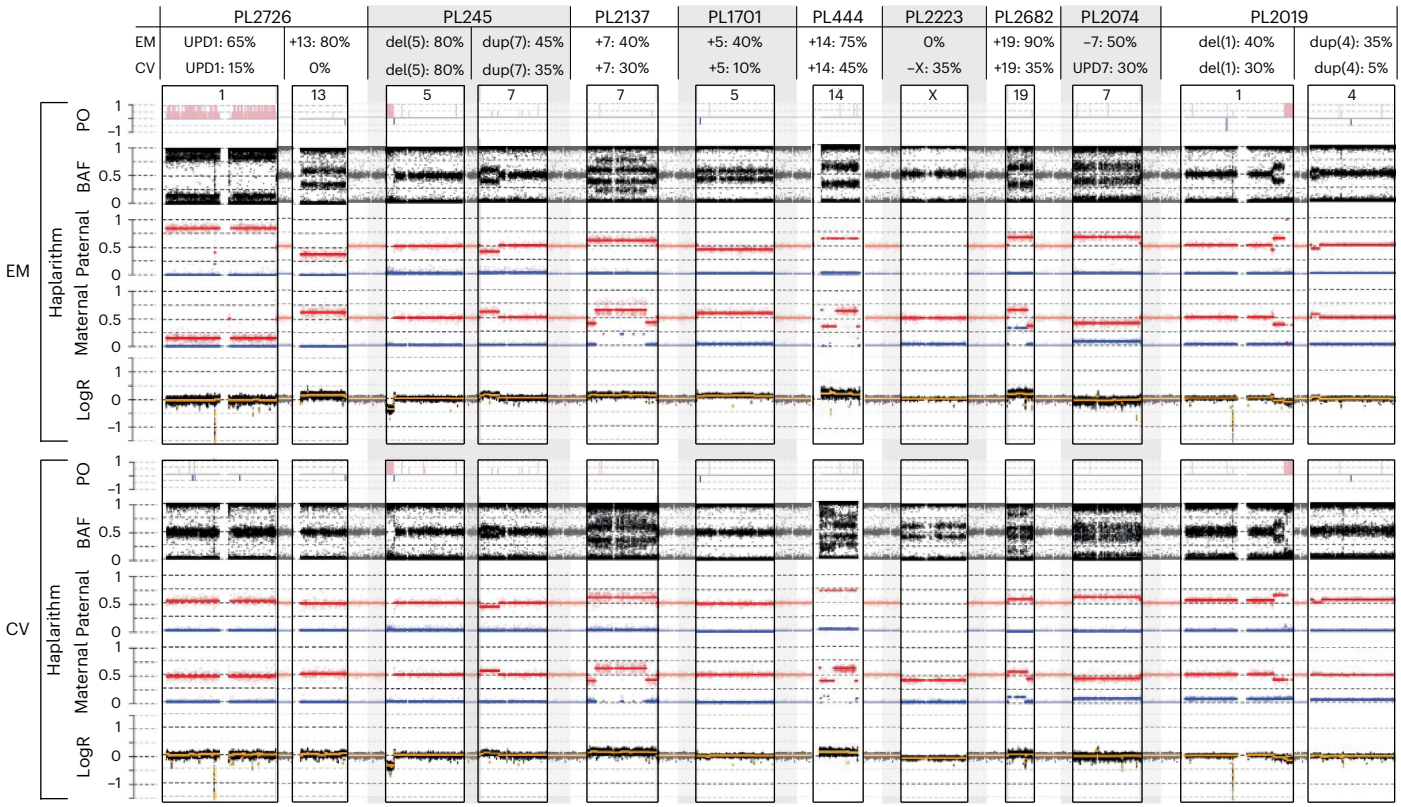


**Fig. 5 | Degree of mosaicism in extra-embryonic mesoderm as compared to chorionic villi.** Haplarithms of nine pregnancy loss samples with differences between extra-embryonic mesoderm (EM) and chorionic villi (CV) of greater than 10% mosaicism. PL2726 has a (EM ~65%, CV ~15%) mosaic UPD 1 of maternal and mitotic origin and an approximately 80% mosaic EM-only trisomy 13 of paternal and mitotic error origin. PL245 has a (EM ~80%, CV ~80%) mosaic (subchromosomal) approximately 16.7-Mb deletion in Chr 5 (p15.1–p15.33) of paternal and mitotic error origin and a (EM ~45%, CV ~35%) mosaic approximately 43.2-Mb duplication in Chr 7 (p14.1–p22.3) of paternal and mitotic error origin. PL2137 has a (EM ~40%, CV ~30%) mosaic trisomy 7 of maternal and mitotic error origin. PL1701 has a (EM ~40%, CV ~10%) mosaic trisomy 5 of paternal and mitotic origin. PL444 has a (EM ~75%, CV ~45%) mosaic trisomy 14 of maternal and meiotic error origin. PL2223 has an approximately 35% mosaic CV-only monosomy X of paternal error origin. PL2682 has a (EM ~90%, CV ~35%) mosaic trisomy 19 of maternal meiotic error origin. PL2074 has an approximately 50% mosaic EM-only monosomy 7 of maternal and mitotic error origin and an approximately 30% mosaic CV-only UPD 7 of maternal and mitotic error origin. PL2019 has a (EM ~40%, CV ~30%) mosaic approximately 44.7-Mb deletion in Chr 1 (q32.1–q44) of paternal and mitotic error origin and a (EM ~35%, CV ~5%) mosaic approximately 18.3-Mb duplication in Chr 4 (p15.32–p16.3) of paternal and mitotic error origin. del, deletion; dup, duplication; Mb, megabase; +, trisomy; −, monosomy; PO, parent-of-origin.

comparing genome haplarithmisis with conventional methods to evaluate its clinical implementation and cost-effectiveness for management of pregnancy loss. The guidelines of the European Society of Human Reproduction and Embryology (ESHRE) in RPL restated the limitation of conventional karyotyping and underscored the importance of future studies that explore the role of next-generation sequencing techniques[56]. A strategy using genetic analysis of miscarriage tissue could help patients deal with the psychological impact of pregnancy loss and would limit the need for further expensive and elaborate maternal investigations for other causes of RPL[57].

Profiling the genomic landscape of pregnancy losses by carefully dissecting both the extra-embryonic mesoderm and chorionic villi tissues of the same POC and applying haplarithmisis allowed us to detect and classify 35.1% of karyotypically normal POCs as abnormal. Moreover, POCs with different levels of mosaicism in extra-embryonic mesoderm and chorionic villi were found, with the prevalence of aberrations being higher in extra-embryonic mesoderm compared to chorionic villi. This finding raises intriguing hypotheses about the origins of mosaic mutations in pregnancy loss. Although extra-embryonic mesoderm develops before gastrulation in primates, it develops during gastrulation in rodents. Therefore, extra-embryonic mesoderm cells are most likely derived from transient primary yolk sac, which is of embryoblast, and not trophoblast, origin[35]. It was previously suggested that self-correction mechanisms for aneuploidy are active in the inner cell mass during early embryogenesis and that there is a selective bottleneck in early embryogenesis when aneuploid cells are depleted[11,12]. Our data are compatible with a selective scenario in which chromosomal aberrations first emerge in the inner cell mass of the blastocyst and persist at least in extra-embryonic mesoderm, conferring a strong detrimental effect on the pregnancy outcome, which may result in pregnancy loss.

We found that SPL and RPL cohorts have similar prevalence of genomic aberrations. However, these two groups had different types of genomic aberrations, such that the SPL cohort had significantly more segmental aberrations, whereas the RPL cohort carried more aneuploidies (Fig. 1c). Although our cohort is underpowered to draw firm conclusions, our POC analysis points to possible differences in the genetic etiology of pregnancy losses, which merits further study. We emphasize the importance of reaching an international consensus on the clinical definition of RPL, which is the topic of an ongoing debate and differs across guidelines and countries[1,56]. ESHRE's guidelines from 2022 define RPL as the loss of two or more pregnancies before 24 weeks of gestation[56], which was used in the present study.

Our data inform discussions about the clinical importance of scrutinizing the full allelic architecture of genomic abnormalities and their segregational origin (meiotic versus mitotic origin) in human

embryos and pregnancies with relevance for the safety of transferring in vitro fertilized (IVF) embryos with mosaic imbalances[58] as well as interpretation of NIPT results with mosaic aberration indications. In nationwide NIPT studies[31,32], the rate of confirmed confined fetal mosaicism is very low compared to confined placental mosaicism, indicating that abnormal cells in the fetus are less tolerated relative to the placenta. For instance, 94% of rare autosomal trisomies in NIPT were found to be most likely due to confined placental mosaicism[31]. The impact of chromosomal mosaicism is less clear due to current limitations for its detection. According to some rare cytogenetic studies on spontaneous pregnancy losses and confined placental chromosomal mosaicism, confined placental mosaicism is found in approximately 20% of the POCs, which is higher than the reported rate of 1–2% seen in viable pregnancies in chorionic villus sampling[53,59–61]. Additionally, when we compared the nature and prevalence of genomic aberrations along the gestational weeks of the first trimester, we observed that, on average, there may be a higher level of mosaicism in earlier POCs (Supplementary Tables 2 and 5). For instance, for mitotic aberrations in extra-embryonic mesoderm ($n = 14$), the average level of mosaicism in POCs of gestational weeks 4–7 ($n = 7$) was 67.9% ± 26.4 s.d., whereas, in POCs of gestational weeks 8–13 ($n = 7$), the average level of mosaicism was 48.9% ± 30.8 s.d. ($P = 0.33$, two-sided Mann–Whitney $U$-test; Supplementary Table 5). Our cohort is underpowered to draw firm conclusions regarding the comparison of different gestational ages. To reach a sufficient power of 0.8, a minimum sample size of 86—that is, 43 POCs per time interval—would be required (Methods). In addition, a complete allelic architecture of pregnancy loss in the second and third trimesters in future studies will reveal a more detailed etiology of pregnancy losses that are caused by pre-zygotic or post-zygotic chromosomal alterations.

This study has practical implications, contributing to the emerging studies using NIPT in RPL[62]. Specifically, in the case of detected copy number changes after NIPT, genome haplarithmisis can distinguish between meiotic and mitotic errors. NIPT with confined placental mosaicism can lead to false-positive test results. These findings require fetal invasive genetic testing that could potentially be avoided by accurate detection of the segregational origin of the mutation as well as linking low abundant cell-free DNA (cfDNA) to the fetal or placental lineage, which is required to exclude the presence of aberrant cells in the fetus. Aberrations of meiotic origin, if occurring via rescue events into mosaic blastocysts, are likely affecting both fetal and placental lineages and predisposing for spontaneous miscarriage, whereas mitotic aberrations may be specific to the placenta due to confined placental mosaicism[10] and are compatible with healthy pregnancies. This allows differentiating low-risk pregnancy aneuploidies with aneuploidies of mitotic origin where the fetus may not be affected from higher-risk pregnancies with severe clinical consequences where the fetus is likely affected, as meiotic aberrations are present in both the fetal and placental lineages. Additionally, epigenetic studies of cfDNA have suggested that fetal tissues other than the placenta-derived trophoblasts may also contribute to the cfDNA mixture of maternal blood[63]. This makes it possible to differentiate confined placental mosaicism, which is apparently safe for pregnancy, from a situation where (mosaic) aberration is present in both placental tissue and the fetus, with a higher risk for pregnancy loss. This underlines the importance of developing technologies that can reliably identify placental and fetal origin when an aberration is found in early pregnancy. Moreover, haplotyping-based NIPT methods enable a generic approach for detection of monogenic disorders[64].

Taken together, the detection of the segregational origin of chromosomal aberrations is of paramount importance for prognosing the successful completion of pregnancy. Although embryos with mosaic abnormalities can lead to the birth of healthy babies[65], the meiotic or mitotic origin of mosaicism has not always been determined in these successful cases. For instance, as in PGT of IVF embryos, the DNA sample is derived from a single trophectoderm biopsy, and the true extent of mosaicism in all embryo compartments, including the inner cell mass, cannot be determined. However, the determination of the segregational origin of mosaic aberrations would help to avoid transferring meiotic (mosaic) IVF embryos, which confer a high risk for inner cell mass aberrations and later pregnancy loss. In contrast, we suggest that the rules for selecting mitotic mosaic embryos for uterine transfer could be more relaxed.

In conclusion, our study shows that as many as two-thirds of all pregnancy losses may be due to fetal chromosomal abnormalities. Furthermore, the ability to accurately determine the segregational and lineage origins of fetal genomic aberrations may enhance the efficacy of human natural and assisted conception and, thereby, improve reproductive genetic care in general.

## Online content

Any methods, additional references, Nature Portfolio reporting summaries, source data, extended data, supplementary information, acknowledgements, peer review information; details of author contributions and competing interests; and statements of data and code availability are available at https://doi.org/10.1038/s41591-023-02645-5.

## References


1. Quenby, S. et al. Miscarriage matters: the epidemiological, physical, psychological, and economic costs of early pregnancy loss. *Lancet* **397**, 1658–1667 (2021).
2. Coomarasamy, A. et al. Sporadic miscarriage: evidence to provide effective care. *Lancet* **397**, 1668–1674 (2021).
3. Gruhn, J. R. et al. Chromosome errors in human eggs shape natural fertility over reproductive life span. *Science* **365**, 1466–1469 (2019).
4. Hassold, T. et al. Failure to recombine is a common feature of human oogenesis. *Am. J. Hum. Genet.* **108**, 16–24 (2021).
5. Starostik, M. R., Sosina, O. A. & McCoy, R. C. Single-cell analysis of human embryos reveals diverse patterns of aneuploidy and mosaicism. *Genome Res.* **30**, 814–825 (2020).
6. Vanneste, E. et al. Chromosome instability is common in human cleavage-stage embryos. *Nat. Med.* **15**, 577–583 (2009).
7. Zamani Esteki, M. et al. Concurrent whole-genome haplotyping and copy-number profiling of single cells. *Am. J. Hum. Genet.* **96**, 894–912 (2015).
8. Charalambous, C., Webster, A. & Schuh, M. Aneuploidy in mammalian oocytes and the impact of maternal ageing. *Nat. Rev. Mol. Cell Biol.* **24**, 27–44 (2023).
9. Palmerola, K. L. et al. Replication stress impairs chromosome segregation and preimplantation development in human embryos. *Cell* **185**, 2988–3007 (2022).
10. Zamani Esteki, M. et al. In vitro fertilization does not increase the incidence of de novo copy number alterations in fetal and placental lineages. *Nat. Med.* **25**, 1699–1705 (2019).
11. Yang, M. et al. Depletion of aneuploid cells in human embryos and gastruloids. *Nat. Cell Biol.* **23**, 314–321 (2021).
12. Orvieto, R. et al. Do human embryos have the ability of self-correction? *Reprod. Biol. Endocrinol.* **18**, 98 (2020).
13. Lebedev, I. Mosaic aneuploidy in early fetal losses. *Cytogenet. Genome Res.* **133**, 169–183 (2011).
14. Grati, F. R. et al. Fetoplacental mosaicism: potential implications for false-positive and false-negative noninvasive prenatal screening results. *Genet. Med.* **16**, 620–624 (2014).
15. Byrne, A. B. et al. Genomic autopsy to identify underlying causes of pregnancy loss and perinatal death. *Nat. Med.* **29**, 180–189 (2023).
16. Nybo Andersen, A. M., Wohlfahrt, J., Christens, P., Olsen, J. & Melbye, M. Maternal age and fetal loss: population based register linkage study. *BMJ* **320**, 1708–1712 (2000).

17. Magnus, M. C., Wilcox, A. J., Morken, N. H., Weinberg, C. R. & Haberg, S. E. Role of maternal age and pregnancy history in risk of miscarriage: prospective register based study. *BMJ* **364**, l869 (2019).
18. Hassold, T. & Hunt, P. To err (meiotically) is human: the genesis of human aneuploidy. *Nat. Rev. Genet.* **2**, 280–291 (2001).
19. Conlin, L. K. et al. Mechanisms of mosaicism, chimerism and uniparental disomy identified by single nucleotide polymorphism array analysis. *Hum. Mol. Genet.* **19**, 1263–1275 (2010).
20. Hardy, K., Hardy, P. J., Jacobs, P. A., Lewallen, K. & Hassold, T. J. Temporal changes in chromosome abnormalities in human spontaneous abortions: results of 40 years of analysis. *Am. J. Med. Genet. A* **170**, 2671–2680 (2016).
21. Levy, B. et al. Genomic imbalance in products of conception: single-nucleotide polymorphism chromosomal microarray analysis. *Obstet. Gynecol.* **124**, 202–209 (2014).
22. Zhou, Q., Wu, S. Y., Amato, K., DiAdamo, A. & Li, P. Spectrum of cytogenomic abnormalities revealed by array comparative genomic hybridization on products of conception culture failure and normal karyotype samples. *J. Genet. Genomics* **43**, 121–131 (2016).
23. Chen, Y. et al. Characterization of chromosomal abnormalities in pregnancy losses reveals critical genes and loci for human early development. *Hum. Mutat.* **38**, 669–677 (2017).
24. Li, F. X. et al. Detection of chromosomal abnormalities in spontaneous miscarriage by low-coverage next-generation sequencing. *Mol. Med. Rep.* **22**, 1269–1276 (2020).
25. Peng, J. P. & Yuan, H. M. [Application of chromosomal microarray analysis for a cohort of 2600 Chinese patients with miscarriage]. *Yi Chuan* **40**, 779–788 (2018).
26. Wang, Y. et al. Identification of chromosomal abnormalities in early pregnancy loss using a high-throughput ligation-dependent probe amplification-based assay. *J. Mol. Diagn.* **23**, 38–45 (2021).
27. Finley, J. et al. The genomic basis of sporadic and recurrent pregnancy loss: a comprehensive in-depth analysis of 24,900 miscarriages. *Reprod. Biomed. Online* **45**, 125–134 (2022).
28. Sahoo, T. et al. Comprehensive genetic analysis of pregnancy loss by chromosomal microarrays: outcomes, benefits, and challenges. *Genet. Med.* **19**, 83–89 (2017).
29. Peng, G. et al. Estimation on risk of spontaneous abortions by genomic disorders from a meta-analysis of microarray results on large case series of pregnancy losses. *Mol. Genet. Genomic Med.* **11**, e2181 (2023).
30. Van Prooyen Schuurman, L. et al. Clinical impact of additional findings detected by genome-wide non-invasive prenatal testing: follow-up results of the TRIDENT-2 study. *Am. J. Hum. Genet.* **109**, 1140–1152 (2022).
31. van der Meij, K. R. M. et al. TRIDENT-2: national implementation of genome-wide non-invasive prenatal testing as a first-tier screening test in the Netherlands. *Am. J. Hum. Genet.* **105**, 1091–1101 (2019).
32. Van Den Bogaert, K. et al. Outcome of publicly funded nationwide first-tier noninvasive prenatal screening. *Genet. Med.* **23**, 1137–1142 (2021).
33. Tsuiko, O. et al. Haplotyping-based preimplantation genetic testing reveals parent-of-origin specific mechanisms of aneuploidy formation. *NPJ Genom. Med.* **6**, 81 (2021).
34. Capalbo, A. et al. Mosaic human preimplantation embryos and their developmental potential in a prospective, non-selection clinical trial. *Am. J. Hum. Genet.* **108**, 2238–2247 (2021).
35. Ross, C. & Boroviak, T. E. Origin and function of the yolk sac in primate embryogenesis. *Nat. Commun.* **11**, 3760 (2020).
36. Boss, A. L., Chamley, L. W. & James, J. L. Placental formation in early pregnancy: how is the centre of the placenta made? *Hum. Reprod. Update* **24**, 750–760 (2018).
37. Kolte, A. M., Westergaard, D., Lidegaard, O., Brunak, S. & Nielsen, H. S. Chance of live birth: a nationwide, registry-based cohort study. *Hum. Reprod.* **36**, 1065–1073 (2021).
38. Bortoletto, P. et al. Miscarriage syndrome: linking early pregnancy loss to obstetric and age-related disorders. *EBioMedicine* **81**, 104134 (2022).
39. Shimokawa, O. et al. Array comparative genomic hybridization analysis in first-trimester spontaneous abortions with 'normal' karyotypes. *Am. J. Med. Genet. A* **140**, 1931–1935 (2006).
40. Zhang, Y. X. et al. Genetic analysis of first-trimester miscarriages with a combination of cytogenetic karyotyping, microsatellite genotyping and arrayCGH. *Clin. Genet.* **75**, 133–140 (2009).
41. Warren, J. E., Turok, D. K., Maxwell, T. M., Brothman, A. R. & Silver, R. M. Array comparative genomic hybridization for genetic evaluation of fetal loss between 10 and 20 weeks of gestation. *Obstet. Gynecol.* **114**, 1093–1102 (2009).
42. Rajcan-Separovic, E. et al. Identification of copy number variants in miscarriages from couples with idiopathic recurrent pregnancy loss. *Hum. Reprod.* **25**, 2913–2922 (2010).
43. Kooper, A. J., Faas, B. H., Feenstra, I., de Leeuw, N. & Smeets, D. F. Best diagnostic approach for the genetic evaluation of fetuses after intrauterine death in first, second or third trimester: QF-PCR, karyotyping and/or genome wide SNP array analysis. *Mol. Cytogenet.* **7**, 6 (2014).
44. Bug, S. et al. Diagnostic utility of novel combined arrays for genome-wide simultaneous detection of aneuploidy and uniparental isodisomy in losses of pregnancy. *Mol. Cytogenet.* **7**, 43 (2014).
45. Robberecht, C., Schuddinck, V., Fryns, J. P. & Vermeesch, J. R. Diagnosis of miscarriages by molecular karyotyping: benefits and pitfalls. *Genet. Med.* **11**, 646–654 (2009).
46. Takahara, H., Ohama, K. & Fujiwara, A. Cytogenetic study in early spontaneous abortion. *Hiroshima J. Med. Sci.* **26**, 291–296 (1977).
47. Hassold, T. et al. A cytogenetic study of 1000 spontaneous abortions. *Ann. Hum. Genet.* **44**, 151–178 (1980).
48. Kajii, T. et al. Anatomic and chromosomal anomalies in 639 spontaneous abortuses. *Hum. Genet.* **55**, 87–98 (1980).
49. Byrne, J., Warburton, D., Kline, J., Blanc, W. & Stein, Z. Morphology of early fetal deaths and their chromosomal characteristics. *Teratology* **32**, 297–315 (1985).
50. Lin, C. C., De Braekeleer, M. & Jamro, H. Cytogenetic studies in spontaneous abortion: the Calgary experience. *Can. J. Genet. Cytol.* **27**, 565–570 (1985).
51. Dejmek, J., Vojtassak, J. & Malova, J. Cytogenetic analysis of 1508 spontaneous abortions originating from south Slovakia. *Eur. J. Obstet. Gynecol. Reprod. Biol.* **46**, 129–136 (1992).
52. Be, C., Velasquez, P. & Youlton, R. [Spontaneous abortion: cytogenetic study of 609 cases]. *Rev. Med. Chil.* **125**, 317–322 (1997).
53. Griffin, D. K., Millie, E. A., Redline, R. W., Hassold, T. J. & Zaragoza, M. V. Cytogenetic analysis of spontaneous abortions: comparison of techniques and assessment of the incidence of confined placental mosaicism. *Am. J. Med. Genet.* **72**, 297–301 (1997).
54. Brajenovic-Milic, B., Petrovic, O., Krasevic, M., Ristic, S. & Kapovic, M. Chromosomal anomalies in abnormal human pregnancies. *Fetal Diagn. Ther.* **13**, 187–191 (1998).
55. Qumsiyeh, M. B., Kim, K. R., Ahmed, M. N. & Bradford, W. Cytogenetics and mechanisms of spontaneous abortions: increased apoptosis and decreased cell proliferation in chromosomally abnormal villi. *Cytogenet. Cell Genet.* **88**, 230–235 (2000).
56. European Society of Human Reproduction and Embryology. *Recurrent Pregnancy Loss Guideline of European Society of Human Reproduction and Embryology* (European Society of Human Reproduction and Embryology, 2022).

57. Popescu, F., Jaslow, C. R. & Kutteh, W. H. Recurrent pregnancy loss evaluation combined with 24-chromosome microarray of miscarriage tissue provides a probable or definite cause of pregnancy loss in over 90% of patients. *Hum. Reprod.* **33**, 579–587 (2018).
58. Mastenbroek, S., De Wert, G. & Adashi, E. Y. The imperative of responsible innovation in reproductive medicine. *N. Engl. J. Med.* **385**, 2096–2100 (2021).
59. Kalousek, D. K., Barrett, I. J. & Gartner, A. B. Spontaneous abortion and confined chromosomal mosaicism. *Hum. Genet.* **88**, 642–646 (1992).
60. Lebedev, I. N., Ostroverkhova, N. V., Nikitina, T. V., Sukhanova, N. N. & Nazarenko, S. A. Features of chromosomal abnormalities in spontaneous abortion cell culture failures detected by interphase FISH analysis. *Eur. J. Hum. Genet.* **12**, 513–520 (2004).
61. Kalousek, D. K. Pathogenesis of chromosomal mosaicism and its effect on early human development. *Am. J. Med. Genet.* **91**, 39–45 (2000).
62. D'Ippolito, S. et al. Investigating the 'fetal side' in recurrent pregnancy loss: reliability of cell-free DNA testing in detecting chromosomal abnormalities of miscarriage tissue. *J. Clin. Med.* **12**, 3898 (2023).
63. Gordevicius, J. et al. Identification of fetal unmodified and 5-hydroxymethylated CG sites in maternal cell-free DNA for non-invasive prenatal testing. *Clin. Epigenetics* **12**, 153 (2020).
64. Che, H. et al. Noninvasive prenatal diagnosis by genome-wide haplotyping of cell-free plasma DNA. *Genet. Med.* **22**, 962–973 (2020).
65. Greco, E., Minasi, M. G. & Fiorentino, F. Healthy babies after intrauterine transfer of mosaic aneuploid blastocysts. *N. Engl. J. Med.* **373**, 2089–2090 (2015).

**Publisher's note** Springer Nature remains neutral with regard to jurisdictional claims in published maps and institutional affiliations.

**Open Access** This article is licensed under a Creative Commons Attribution 4.0 International License, which permits use, sharing, adaptation, distribution and reproduction in any medium or format, as long as you give appropriate credit to the original author(s) and the source, provide a link to the Creative Commons license, and indicate if changes were made. The images or other third party material in this article are included in the article's Creative Commons license, unless indicated otherwise in a credit line to the material. If material is not included in the article's Creative Commons license and your intended use is not permitted by statutory regulation or exceeds the permitted use, you will need to obtain permission directly from the copyright holder. To view a copy of this license, visit http://creativecommons.org/licenses/by/4.0/.

© The Author(s) 2023

[1]Department of Clinical Genetics, Maastricht University Medical Center (MUMC+), Maastricht, The Netherlands. [2]Department of Genetics and Cell Biology, GROW-Research Institute for Oncology and Reproduction, Faculty of Health, Medicine and Life Sciences (FHML), Maastricht University, Maastricht, The Netherlands. [3]Research Institute of Medical Genetics, Tomsk National Research Medical Center of the Russian Academy of Sciences, Tomsk, Russia. [4]Department of Biotechnology, Institute of Molecular and Cell Biology, University of Tartu, Tartu, Estonia. [5]Department of Anatomy & Embryology, Faculty of Health, Medicine and Life Sciences (FHML), Maastricht University, Maastricht, The Netherlands. [6]Department of Clinical Epidemiology and Medical Technology Assessment (KEMTA), Maastricht University Medical Center (MUMC+), Maastricht, The Netherlands. [7]Department of Obstetrics and Gynaecology, Institute of Clinical Medicine, University of Tartu, Tartu, Estonia. [8]Department of Obstetrics and Gynecology, University of Helsinki, Helsinki, Finland. [9]Department of Obstetrics and Gynaecology, Maastricht University Medical Center (MUMC+), Maastricht, The Netherlands. [10]Department of Human Genetics, Radboud University Medical Center, Nijmegen, The Netherlands. [11]Department of Internal Medicine, Center for Infectious Disease (RCI), Radboud University Medical Center, Nijmegen, The Netherlands. [12]Radboud Institute for Molecular Life Sciences, Radboud University Medical Center, Nijmegen, The Netherlands. [13]Radboud Expertise Center for Immunodeficiency and Autoinflammation and Radboud Center for Infectious Disease (RCI), Radboud University Medical Center, Nijmegen, The Netherlands. [14]Competence Center on Health Technologies, Tartu, Estonia. [15]Division of Obstetrics and Gynecology, Department of Clinical Science, Intervention & Technology (CLINTEC), Karolinska Institutet and Karolinska University Hospital, Stockholm, Sweden. [16]These authors contributed equally: Rick Essers, Igor N. Lebedev, Ants Kurg. [17]These authors jointly supervised this work: Andres Salumets, Masoud Zamani Esteki. ✉e-mail: andres.salumets@ki.se; masoud.zamaniesteki@mumc.nl

## Methods

### Ethical approval

Embryonic tissues and parental blood samples were obtained from the Biobank of Populations of Northern Eurasia, Research Institute of Medical Genetics, Tomsk National Research Medical Center. All couples signed an appropriate informed consent for the transfer of their samples to the biobank for scientific research. This study was approved by the local ethics committee of the Research Institute of Medical Genetics, Tomsk National Research Medical Center, of the Russian Academy of Sciences (protocol no. 15 February 2021). Permission was given for the retrospective analysis of the anonymized biological samples of the biobank.

### Ultrasound diagnosis of early pregnancy loss

The ultrasonography features of early pregnancy loss considered in this study were no cardiac activity or empty gestational sac with a diameter ≥25 mm, crown–rump lengths (CRLs) ≥7 mm for embryos with no cardiac activity, the absence of an embryo and its cardiac activity 14 d after the detection of a gestational sac without a yolk sac and the absence of an embryo and its cardiac activity 11 d after the detection of a gestational sac with a yolk sac[66]. Anembryonic pregnancy (AP) was diagnosed in the absence of an embryo in the gestational sac for a period of more than 7 weeks; in addition, ultrasound criteria for AP were a gestational sac ≥13 mm without a yolk sac or ≥18 mm without an embryo. Missed abortion (MA) was diagnosed for embryos with CRL ≥7 mm without cardiac activity or no cardiac activity upon the initial scan and post-7-days scan for embryos with CRL <7 mm. Spontaneous abortion (SA) was diagnosed as a spontaneously terminated pregnancy without ultrasound examination. The most frequent clinical forms of early pregnancy loss in our study were MAs, followed by APs and SAs (Table 1). After ultrasonography diagnosis, women were admitted to gynecological clinics for curettage or medication abortion. Extra-embryonic tissues or fragmented gestational sacs were collected in sterile saline and immediately transferred to the Laboratory of Cytogenetics, Research Institute of Medical Genetics, Tomsk National Research Medical Center, for cytogenetic analysis and cryopreservation.

### Sampling of POCs

The POCs, usually represented by fragments of the gestational sac, were delivered to the laboratory in sterile saline, thoroughly washed and separated from decidual tissues and blood clots under an inverted microscope. Part of each tissue sample was used for cell culture, and the remaining tissue sample was stored at −70 °C for DNA extraction. Traditionally, cytogenetic studies of POCs have used one of two methods to determine the karyotype[53]. The first involves long-term culture of extra-embryonic tissues; most often, cells that are cultured are derived from the stroma of the chorionic villi[47]. The second approach exploits spontaneously and rapidly dividing cells of the cytotrophoblast to obtain direct chromosome preparations without culturing[67,68]. Usually, the results of both techniques are similar. However, discordant results can be obtained in some cases due to tissue-specific placental mosaicism[13]. Therefore, when large fragments of fetal sac were present, the internal mesodermal layer of extra-embryonic membrane was used for cell culture; otherwise, both extra-embryonic mesoderm and chorionic villi were used (see the 'Chorionic villi and extra-embryonic mesoderm dissection of the POCs and DNA extraction' subsection). The tissues were chopped with scissors into small fragments, and long-term cultures were set up in 25-cm$^2$ flasks with 5 ml of DMEM/F12 (1:1) medium (Gibco) supplemented with 20% FBS (HyClone), 1% MEM NEAA solution (Gibco) and 1% penicillin–streptomycin (Gibco). Tissues were incubated at 37 °C with once-weekly medium renewal. Extra-embryonic fibroblasts were cultivated until sufficient mitotic cells for cytogenetic analysis were obtained. Demecolcine (Sigma-Aldrich) was added 4 h before chromosome harvesting, and the samples were processed using standard techniques of hypotonic treatment with 0.55% sodium citrate and cell fixation with a 1:3 mixture of acetic acid:methanol. In some cases, direct preparations of the chorionic villi were used[69]. Slide preparations and GTG banding were performed by standard protocols in accordance with guidelines[70]. Subsequently, frozen tissues were used for DNA extraction and preparation of cell suspensions for interphase FISH.

### Chorionic villi and extra-embryonic mesoderm dissection of the POCs and DNA extraction

Genomic DNA was extracted from blood samples of the parents and from two distinct locations in the POC: chorionic villi and extra-embryonic mesoderm. The dissection of chorionic villi and extra-embryonic mesoderm by an experienced pathologist is possible from the fourth week of gestation onwards, whereas, from the sixth week of gestation, the separation of extra-embryonic mesoderm and chorionic villi almost always succeeds (the mean gestational week in this study is 7.5 ± 1.7 s.d.). Specifically, after thawing, chorionic villi were carefully scraped off under an Axiovert 200 inverted microscope (Carl Zeiss) from extra-embryonic membranes based on their morphology, and DNA was extracted separately from these tissues of each sample. The main limitation for accurate dissection of chorionic villi and extra-embryonic mesoderm, however, is the way that POCs are acquired after pregnancy termination. This is because different methods after pregnancy termination are used in medical practice, including curettage, vacuum aspiration or using specific drugs. Genomic DNA was extracted using a standard phenol–chloroform extraction method that allows for the isolation of up to 900 ng of DNA from the tissues. To isolate DNA from tissues, a small fragment of tissue (200–300 mg) was taken. Then, samples of chorionic villi or extra-embryonic mesoderm were placed in Eppendorf tubes, and 467 µl of buffer (1 ml of 1 M Tris-HCl, pH 7.4; 2 ml of 0.5 M EDTA; 200 µl of 5 M NaCl; 96.8 ml of water) was added to them, in addition to 25 µl of 20% SDS and 7.5 µl of proteinase K (10 mg ml$^{-1}$). The samples were incubated for 16 h at 37 °C. Then, 550 µl of phenol was added, mixed gently and centrifuged for 3 min at 12,000 r.p.m. and room temperature. Next, 300 µl of phenol and 300 µl of a mixture (chloroform:isoamyl alcohol in a ratio of 24:1) were added to the supernatant liquid, mixed and centrifuged under the same conditions. Afterwards, 550 µl of the mixture (chloroform:isoamyl alcohol) was added to the supernatant, mixed and centrifuged. The supernatant liquid was taken again; 30 µl of 10 M sodium acetate and 660 µl of ethanol were added; and the tube was inverted until DNA was visualized. The solution was removed; 100 µl of 70% ethanol was added to the DNA; the DNA was washed and centrifuged at 12,000 r.p.m. for 3 min; the alcohol was removed; and the precipitate was dried at 37 °C. DNA was dissolved in 100 µl of Tris/EDTA buffer. Likewise, genomic DNA was extracted from the peripheral blood of parents using the standard phenol–chloroform method.

### Conventional CGH and interphase FISH

Conventional CGH and interphase FISH with centromere enumeration probes were performed as described previously[60,71] for POC samples where traditional cytogenetic analysis failed. For interphase FISH, two tissues were mechanically separated, and the yield of chorionic cytotrophoblast cells was increased by maceration of chorionic villi under an Axiovert 200 inverted microscope (Carl Zeiss) and treatment with 70% acetic acid for 3–5 min, followed by three washes of the obtained cell suspension with PBS according to a modified protocol[67]. The extra-embryonic mesoderm cells were obtained by digesting the extra-embryonic membrane (Fig. 3a) with 125 U ml$^{-1}$ collagenase type I (Sigma-Aldrich) for 30–60 min at 37 °C (ref. 60). Cell suspensions were fixed and stored in 3:1 methanol:acetic acid at −20 °C. For confirmation studies, interphase FISH was performed separately for thawed chorionic villi and extra-embryonic mesoderm cells using centromere-specific DNA probes for chromosomes 2, 15, X and Y as well as subtelomeric DNA probes for chromosome 16 (16p, 16q). From

100 to 400 interphase nuclei were scored for each sample using an Axio Imager Z2 microscope (Carl Zeiss) with Metafer and ISIS software (MetaSystems).

### Selection criteria for the participating patients

From 1987 to 2021, a total of 1,745 spontaneous pregnancy losses were analyzed using karyotyping. The karyotypes of fetal tissue were determined by conventional metaphase analysis ($n$ = 1,745 and, on average, 10 metaphases) or additional testing by CGH and FISH. All samples with abnormal karyotypes were excluded from downstream haplarithmisis. Of the karyotypically normal cases, 111 families (114 POCs) were randomly selected for SNP haplotyping, given that fetal (extra-embryonic mesoderm and chorionic villi) and parental blood samples were available and that no genetic predisposition for pregnancy loss had been identified in the couple. Twenty families were excluded due to the DNA of one or more family members being of insufficient quantity or quality, causing low SNP call rates or due to one or both parents not being the biological parent, making haplotyping analysis impossible (Supplementary Table 6). Ninety-one families (94 POCs) were successfully analyzed by haplarithmisis. Of those, 42 were categorized as SPL (loss of one pregnancy) and 49 as RPL (loss of two or more consecutive pregnancies).

### Whole-genome SNP genotyping

SNP genotyping was performed on genomic DNA isolates using Illumina Infinium Global-Screening Array-24 version 2.0 and version 3.0 BeadChip Kit (Illumina; Gene Expression Omnibus (GEO) code GLP28939), which contains approximately 665,000 SNP markers with a mean probe spacing of ~4.4 kb and a median probe spacing of ~2.3 kb. Genotype calls, SNP BAF values and logR values of all samples were computed using Illumina GenomeStudio software. Illumina genotyping was performed at the Core Facility of Genomics, Institute of Genomics, University of Tartu, Estonia.

### Genome haplarithmisis

Haplarithmisis is a conceptual workflow that enables simultaneous genome-wide haplotyping and copy number typing using genotyping information from offspring and parents[7]. This originally allowed tracing the inheritance of linked disease variants. Previously, we demonstrated that, using Illumina's Global-Screening Array-24, haplarithmisis can detect low-grade mosaicism (>10%), subchromosomal CNVs (>100 kb), the parental and segregational origin of aberrations and maternal cell contamination in placenta[10].

Specifically, in the present study, the parental genotypes were phased by using the chorionic villi genotype of the POC as a seed for phasing. Subsequently, the BAF values—that is, continuous genotype values (Fig. 2a)—of the extra-embryonic mesoderm and chorionic villi are deduced to parental haplarithms (Fig. 2b). Specifically, (1) informative SNP loci are defined when one parent is heterozygous and the other parent homozygous; and (2) these SNP loci are further categorized into maternal and paternal categories. A paternal category is all the SNP loci that have a heterozygous SNP from the father and a homozygous SNP from the mother. Similarly, a maternal category is all the SNP loci that have heterozygous SNP from the mother and homozygous SNP from the father. Subsequently, (3) a subcategorization is made based on (phased) parental SNP genotype combinations into paternal subcategories P1 and P2 (shown in Fig. 2b) and maternal subcategories M1 and M2 (not shown in Fig. 2b). (4) This results in specific P1 and P2 in paternal haplarithm, depending on homolog inheritance—for example, if homolog 1 (H1) is inherited from the father (and either H1 or H2 from the mother), P1 BAFs are either 0 or 1 (corresponding to homozygous AA and BB genotypes, respectively), and P2 BAFs are 0.5 (corresponding to heterozygous AB genotype). In contrast, when H2 is inherited from the father (and either H1 or H2 from the mother), P1 BAFs are 0.5 (corresponding to heterozygous AB genotype), and P2 BAFs are either 0 or 1 (corresponding to homozygous AA and BB genotypes, respectively). M1 and M2 maternal subcategories are computed in a similar fashion. (5) BAF values are mirrored around the 0.5 axis for SNPs where either parent has a heterozygous SNP call BA after phasing. Thus, if H1 was inherited from the father (and either H1 or H2 from the mother), all P1 BAF values will now have a value of 0, and P2 BAF values will continue to have a value of 0.5. In contrast, if H2 was inherited from the father (and either H1 or H2 from the mother), all P1 BAF values will continue to have a value of 0.5, and all P2 BAF values will now have a value of 1. The same computation applies to P2, M1 and M2 BAFs. Mirroring of these specific values for P1 and P2 allows detection of homologous recombination between the paternal H1 and H2—the same for M1 and M2 maternal subcategories. (6) Per subcategory, consecutive parental BAF values are segmented by piecewise constant fitting (PCF; segmentation parameter gamma set to 14 in this study). (7) The paternal (P1 and P2) and maternal (M1 and M2) segments are visualized into two separate haplarithm plots. Segmented paternal P1 and P2 BAFs are depicted in blue and red, respectively, as are maternal M1 and M2 BAFs in blue and red, respectively. (8) Paternal and maternal haplarithms reveal haplotypes (imbalances) and their parental and segregational origin.

As described previously in detail[7], haplarithmisis has two features for detection of degree of mosaicism (Fig. 2c) and segregational origin (Fig. 2d). First, the parity within each parental haplarithm where the length of P1 and P2 segments should approximately correspond to breakpoints of homolog recombination (similarly for M1 and M2 segments). Second, the reciprocity between parental profiles where the difference between P1 and P2 BAFs ($d_{pat}$) in combination with the difference between M1 and M2 BAFs ($d_{mat}$) is characteristic for specific abnormalities, and their specific pattern correlates to segregational origin. For example, if $d_{pat}$ has a value of 0.67 and $d_{mat}$ has a value of 0.33, and the logR value for this chromosome is raised above 0 (~0.58) as compared to the other chromosomes, this is indicative of a trisomy where the maternal chromosome has an abnormal number of two copies—that is, $1_{paternal}$:$2_{maternal}$ allelic ratio. Subsequently, segregational origin can be determined by the position of the M1 and M2 values around the centromere. These values around the centromere change depending on whether the centromere contains three different homologs (H1 maternal, H2 maternal and H1 paternal, indicating meiosis I) or two different homologs (H1 maternal and H1 paternal, indicating meiosis II or mitosis). To distinguish between meiosis II and mitotic errors, the M1 and M2 values effected by a recombination event are used. This depends on whether there are three different homologs (H1 maternal, H2 maternal and H1 paternal, indicating meiosis II) or two different homologs (H1 maternal and H1 paternal, indicating mitosis) at the recombination event. To determine the degree of mosaicism, the genomic coordinates at the logR distortion from the expected value—that is, logR = 0—were used to extract the BAFs and segmented P1, P2 or M1, M2 BAFs of the location of interest. BAF values were then compared to the reference dataset for calculation of level of mosaicism, as described previously[19].

Haplarithmisis was applied to each quartet DNA sample to delineate the allelic architecture of the fetal tissues. Chorionic villi tissue was used as a reference to phase parental genotypes. Parental haplarithms were used to infer the DNA copy number state, parent of origin and level of mosaicism of fetal tissues. In total, 450 DNA samples were analyzed. Levels of mosaicism were calculated as previously described[19]. Parent-of-origin haplotyping allows for the detection of maternal DNA contribution in fetal tissues, as previously described[10]. In one DNA sample, complete maternal contamination was detected by genome haplarithmisis and validated by quantitative fluorescence polymerase chain reaction (QF–PCR). This DNA sample was excluded from the study.

### Classification of (segmental) chromosomal abnormalities

Haplarithms of analyzed tissues were classified based on several factors: types of aberrations detected, size of aberrations (genome-wide/chromosomal/segmental), placental or embryonic origin based on

tissue biopsy, parental (paternal, maternal) and segregational (mitotic, meiosis I, meiosis II) origin and level (%) of mosaicism. Levels of mosaicism were calculated based on BAF values as previously described[19]. Extrapolation of the total abnormalities was calculated using the formula below:

$$\left(\left(\mathrm{AK}+\left(\frac{\mathrm{NK}\times\mathrm{AH}}{\mathrm{TH}}\right)\right)\times 100\right)/\mathrm{TK}=67.8\%$$

where AK is the number of abnormal cases by conventional karyotyping; NK is the number of normal cases by conventional karyotyping; AH is the number of abnormal cases by genome haplarithmisis; TH is the total number of cases by genome haplarithmisis; and TK is the total number of cases by conventional karyotyping.

### Other statistical analyses

Comparisons between conventional karyotyping ($n$ = 1,745) and genome haplarithmisis ($n$ = 91 families, 94 POCs) concerning parental and gestational age were performed by two-sided Welch's $t$-test. For dichotomous outcomes, the chi-squared test was applied to analyze parental and segregational origin outcomes of SPL and RPL. Due to low sample size (non-parametric) and paired samples (extra-embryonic mesoderm and chorionic villi from a single fetus), the Wilcoxon signed-rank test was applied to assess the difference in mosaicism degree between extra-embryonic mesoderm and chorionic villi. To calculate the required sample size for the Wilcoxon signed-rank test for matched pairs to test the difference in mosaicism between extra-embryonic mesoderm and chorionic villi, we assumed a normal parent distribution, a mean percentage of 43% mosaicism in the chorionic villi group, an s.d. of 30 in both groups and a correlation between the groups of 0.5. A total sample size of 35 participants was required to test a 15% difference between the extra-embryonic mesoderm and chorionic villi groups, performing a two-sided test using an alpha of 0.05 and a power (1-β) of 0.80. The sample size calculation was performed using G*Power 3.1.9.7. In addition, a power calculation was performed for mosaicism dynamics across gestational age bins. A total sample size of 86 samples was required to test a 15% difference between week bins 4–7 ($n$ = 7) and 8–13 ($n$ = 7) for extra-embryonic mesoderm tissues containing aberrations of mitotic origin, performing a two-sided test using an alpha of 0.05 and a power of (1-β) of 0.80, indicating that our study is underpowered concerning mosaicism dynamics across gestational age, with a power of (1-β) of 0.18 due to low sample size (Supplementary Tables 2 and 5). To assess the relation between mosaicism and gestational age week bins (4–7 and 8–13), two-sided Mann–Whitney $U$-test was performed (Supplementary Table 5).

### Methylation profiling: sample selection and processing

For the methylome analysis, seven POCs (13 DNA samples) were randomly selected based on the following inclusion criteria: (1) availability of sufficient extracted DNA; (2) female sex (to eliminate potential sex differences from the analysis); and (3) absence of chromosomal abnormalities according to haplarithmisis. Extracted DNA from both chorionic villi and extra-embryonic mesoderm tissues was processed as follows: 300 ng of DNA from each sample was bisulfite converted using the EZ DNA Methylation Kit (Zymo Research) according to the manufacturer's instructions and analyzed using the Illumina Infinium MethylationEPIC version 1.0 BeadChip Kit (Illumina; GEO code: GLP21145), thereby allowing us to examine DNA methylation at more than 850,000 CpG sites across the human genome. The Illumina methylation array was performed at the Core Facility of Genomics, Institute of Genomics, University of Tartu, Estonia.

### Methylation data processing and analysis

Data pre-processing was carried out using the RnBeads R package as previously described[72,73]. In brief, the data were normalized with subset-quantile within array normalization (SWAN)[74], and poor-quality sites and samples were removed based on the Greedycut algorithm (detection $P$ value threshold: 0.05). The following additional sites were removed: (1) sites on the sex chromosomes, (2) sites near SNPs, (3) sites with missing values in more than 10% of samples and (4) sites not in a CpG context. Additional sample quality control—namely, sex prediction and SNP probe analysis—was carried out using the sEst[75] package and RnBeads, respectively. Methylation beta values, representing the methylated signal intensity divided by the sum of the methylated and unmethylated signal intensity, were used for all analyses. Cellular deconvolution of the samples was performed using the reference-based Houseman algorithm[76] on data pre-processed with the recommended preprocessNoob[77] method and implemented using the minfi[78] package. For this, the reference site and cell type data for stromal, Hofbauer, endothelial, trophoblast, syncytiotrophoblast and nucleated red blood cells (NRBCs) provided by Yuan et al.[79] were used. Welch's $t$-tests were applied for statistical comparison of the cellular proportions predicted in extra-embryonic mesoderm and chorionic villi samples. All high-quality samples and CpG sites were used to conduct a PCA in which beta values were centered but not scaled. The significance of the associations between the principal components (PCs) and sample features was tested as follows: (1) permutation tests (with 10,000 permutations) for continuous numerical variables (gestational age, stromal cells, Hofbauer cells, endothelial cells, NRBCs and syncytiotrophoblast cells) and (2) two-sided Wilcoxon rank tests for binary categorical variables (tissue type).

### RT–qPCR validation of PL2074 monosomy and uniparental disomy

The haplarithm of PL2074 shows 50% mosaic monosomy 7 in the extra-embryonic mesoderm and 30% uniparental disomy (UPD) in the chorionic villi. To validate these findings, RT–qPCR was performed with a diploid control, a hemizygous deletion case, two times diluted DNA from the hemizygous deletion case and extra-embryonic mesoderm and chorionic villi from PL2074. Primers for exon 16 of the *WDR60* gene, which is located at 7q36.3, were used. The reference gene was *HEXB*, which encodes the β subunit of hexosaminidase and is located at 5q13. Reference genomic DNA was obtained from the peripheral blood lymphocytes of a healthy donor. The results confirmed the diploid genome in chorionic villi and the mosaic monosomy in extra-embryonic mesoderm (Extended Data Fig. 6a,b). The combination of monosomy and UPD may be indicative of monosomy rescue where the single homolog is duplicated (Extended Data Fig. 6c).

### RT–qPCR validation of PL1758 and segregational origin of aberrations

The haplarithm of PL1758 shows a genome-wide triploidy of maternal error origin, with mosaic tetrasomy of Chr 2 and Chr 7. The segregational origin appears to be mitotic (Chrs 1, 4 and 12) or meiotic II (Chrs 3, 5, 6, 8, 9, 10, 11, 13, 14, 15, 16, 17, 18, 19, 20, 21 and 22). To validate whether haplotyping with chorionic villi as a reference for extra-embryonic mesoderm would yield accurate parent-of-origin results, additional haplotyping with two different siblings and grandparents from the maternal side as references was performed. The results from PL1758 confirm the segregational origin of the aberrations, even when chorionic villi is used as a reference (Extended Data Fig. 7). RT–qPCR with reference DNA from spontaneous pregnancy loss with 69,XXX karyotype and primers for exon 12 of the *MBD5* gene (2q23.1), exon 12 of the *ASXL2* gene (2p23.3) and exon 1 of the *CHCHD2* gene (7p11.2) were used to confirm tetrasomy for Chr 2 and Chr 7 in DNA from chorionic villi of PL1758. The following calculations and formulas were used to determine the fold change between the copy number of the test loci in the pregnancy loss and reference DNA: average value for three $C_T$; logQT test primer = ($C_T$ test DNA − $C_T$ reference DNA) / slope test primer; (logQT test primer − log QT control primer); fold change = $10^{\text{logQT test primer} - \text{logQT control primer}}$.

Fold change values were used to build a chart (Extended Data Fig. 7b–d). Usually, fold change for reference DNA is 1—namely, there are two copies of the product for reference DNA. Variation from 0.8 to 1.2 in test DNA corresponds to two copies of DNA. Variation from 0.3 or lower to 0.7 (average 0.5–1 copy against two copies) indicates deletion, and variation from 1.3 to 1.7 (average 1.5–3 copies against two copies) indicates duplication. If both reference and test DNA are triploid, and there is a tetrasomy for some chromosome in the test DNA, then the fold change should be approximately 1.33 (that is, four copies against three).

### Short tandem repeat analysis

To confirm relationships and exclude maternal cell contamination, analysis of short tandem repeats (STRs) was carried out using the COrDIS EXPERT 26 Kit for DNA identification of 26 STR markers (Gordiz). The analysis included identification of 26 loci: *AMEL*, *SRY*, *D3S1358*, *TH01*, *D12S391*, *D5S818*, *TPOX*, *Yindel*, *D2S441*, D7S820, *D13S317*, *FGA*, *D22S1045*, *D18S51*, *D16S539*, *D8S1179*, *CSF1PO*, *D6S1043*, *VWA*, *D21S11*, *SE33*, *D10S1248*, *D1S1656*, *D19S433*, *D2S1338* and *DYS391*. PCR products were fractionated using an ABI PRISM 3130 HID capillary electrophoresis system (Applied Biosystems). Fragment length was determined using internal length standards (Size Standard GeneScan 550) and GeneMapper 4.1 software.

### Comparative genomic hybridization array for aneuploidy detection

Chorionic villi DNA samples from SAs and control male and female DNA samples were labeled by a SureTag Labeling Kit (G9502A, Agilent) and purified by SureTag Purification Columns (5190-7730, Agilent). Labeled DNA samples were hybridized using the GenetiSure Pre-Screen Complete Kit (8 × 60K) (G5963A, Agilent) at 67 °C for 24 h, according to the manufacturer's protocol. Microarray images were obtained using a SureScan Microarray Scanner (Agilent) and analyzed by Agilent Feature Extraction (version 12.2.0.7) and CytoGenomics software (version 5.2).

### Reporting summary

Further information on research design is available in the Nature Portfolio Reporting Summary linked to this article.

## Data availability

All SNP array and methylation data generated in this study were deposited in the National Center for Biotechnology Information's Gene Expression Omnibus (http://www.ncbi.nlm.nih.gov/geo/) under accession code GSE228151. Source data are provided with this paper.

## Code availability

Custom code is available on GitHub: https://github.com/CellularGenomicMedicine/Pregnancy_loss_study.

## References


66. Doubilet, P. M. et al. Diagnostic criteria for nonviable pregnancy early in the first trimester. *N. Engl. J. Med.* **369**, 1443–1451 (2013).
67. Simoni, G. et al. Efficient direct chromosome analyses and enzyme determinations from chorionic villi samples in the first trimester of pregnancy. *Hum. Genet.* **63**, 349–357 (1983).
68. Eiben, B. et al. Cytogenetic analysis of 750 spontaneous abortions with the direct-preparation method of chorionic villi and its implications for studying genetic causes of pregnancy wastage. *Am. J. Hum. Genet.* **47**, 656–663 (1990).
69. Kuznetzova, T. V., Trofimova, I. L., Liapunov, M. S., Evdokimenko, E. V. & Baranov, V. S. Selective staining of pericentromeric heterochromatin regions in chromosomes of spontaneously dividing cells with the use of the acridine orange fluorochrome. *Genetika* **48**, 451–456 (2012).
70. Silva, M. et al. European guidelines for constitutional cytogenomic analysis. *Eur. J. Hum. Genet.* **27**, 1–16 (2019).
71. Ostroverkhova, N. V. et al. Detection of aneuploidy in spontaneous abortions using the comparative hybridization method. *Genetika* **38**, 1690–1698 (2002).
72. Muller, F. et al. RnBeads 2.0: comprehensive analysis of DNA methylation data. *Genome Biol.* **20**, 55 (2019).
73. Koeck, R. M. et al. Methylome-wide analysis of IVF neonates that underwent embryo culture in different media revealed no significant differences. *NPJ Genom. Med.* **7**, 39 (2022).
74. Maksimovic, J., Gordon, L. & Oshlack, A. SWAN: subset-quantile within array normalization for Illumina Infinium HumanMethylation450 BeadChips. *Genome Biol.* **13**, R44 (2012).
75. Jung, C. H. et al. sEst: accurate sex-estimation and abnormality detection in methylation microarray data. *Int. J. Mol. Sci.* **19**, 3172 (2018).
76. Houseman, E. A. et al. DNA methylation arrays as surrogate measures of cell mixture distribution. *BMC Bioinformatics* **13**, 86 (2012).
77. Triche, T. J., Weisenberger, D. J., Van Den Berg, D., Laird, P. W. & Siegmund, K. D. Low-level processing of Illumina Infinium DNA methylation beadarrays. *Nucleic Acids Res.* **41**, e90 (2013).
78. Aryee, M. J. et al. Minfi: a flexible and comprehensive bioconductor package for the analysis of Infinium DNA methylation microarrays. *Bioinformatics* **30**, 1363–1369 (2014).
79. Yuan, V. et al. Cell-specific characterization of the placental methylome. *BMC Genomics* **22**, 6 (2021).


## Acknowledgements

We are grateful to all families that participated in this study. We thank all the physicians and cytogeneticists who were involved in ultrasound examination of pregnant women and their genetic counseling, recruiting patients and collecting samples over 35 years. We would like to thank G. Mommen for her contribution to embryo gastrulation illustrations. This study was supported by a Horizon 2020 innovation grant (ERIN, grant no. EU952516) and Horizon Europe (NESTOR, grant no. 101120075) of the European Commission to A.S. and M.Z.E.; the Estonian Research Council (grant no. PRG1076); Enterprise Estonia (grant no. EU48695) to A.S.; the Russian Science Foundation (grant no. 21-65-00017, for cytogenetic analysis, aCGH, STR and RT–qPCR studies of POCs) to I.N.L.; and the Erfelijkheid Voortplanting & Aanleg (EVA) specialty program (grant no. KP111513) of Maastricht University Medical Center to M.Z.E.

## Author contributions

R.E., I.N.L., A.K., A.S. and M.Z.E. conceived the study and designed the experiments. R.E., I.N.L., A.K., S.J.C.S., R.K., U.v.R., S.A.-N., M.V.E.M., A.v.d.W., A.H., H.G.B., A.S. and M.Z.E contributed to manuscript writing and data interpretation. T.V.N., E.A.F., E.A.S. and E.N.T carried out sample collection. T.V.N., E.A.S. and E.N.T. carried out the conventional cytogenetic diagnosis of pregnancy loss. T.V.N., E.A.F. and V.V.D. carried out dissection of chorionic villi and extra-embryonic mesoderm and DNA extraction from fetal tissues and parental blood samples. D.I.Z., G.V.D. and V.V.D. performed conventional CGH, array CGH and interphase FISH. A.A.K., D.A.F. and E.A.F. performed RT–qPCR and STR analysis. A.K. and S.P.D. performed whole-genome SNP genotyping. R.E. and M.Z.E. performed genome haplarithmisis. R.E., S.J.C.S., J.D., A.P., A.H., H.G.B. and M.Z.E. analyzed and interpreted haplarithmisis data. R.E., L.B. and M.Z.E. applied and described statistical analysis. R.E., R.K. and M.Z.E. performed methylation profiling, processing and analysis. A.S. and M.Z.E. oversaw and supervised the study. All authors read and approved the manuscript for submission.

## Competing interests

M.Z.E. is a co-inventor on patent applications ZL910050-PCT/EP2011/060211-WO/2011/157846, 'Methods for haplotyping single cells', and

ZL913096-PCT/EP2014/068315-WO/2015/028576, 'Haplotyping and copy-number typing using polymorphic variant allelic frequencies'. The other authors declare no competing interests.

## Additional information

**Extended data** is available for this paper at https://doi.org/10.1038/s41591-023-02645-5.

**Supplementary information** The online version contains supplementary material available at https://doi.org/10.1038/s41591-023-02645-5.

**Correspondence and requests for materials** should be addressed to Andres Salumets or Masoud Zamani Esteki.

**Peer review information** *Nature Medicine* thanks Mary Norton, Chun So and the other, anonymous, reviewer(s) for their contribution to the peer review of this work. Primary Handling Editor: Sonia Muliyil, in collaboration with the *Nature Medicine* team.

**Reprints and permissions information** is available at www.nature.com/reprints.

https://doi.org/10.1038/s41591-023-02645-5

a

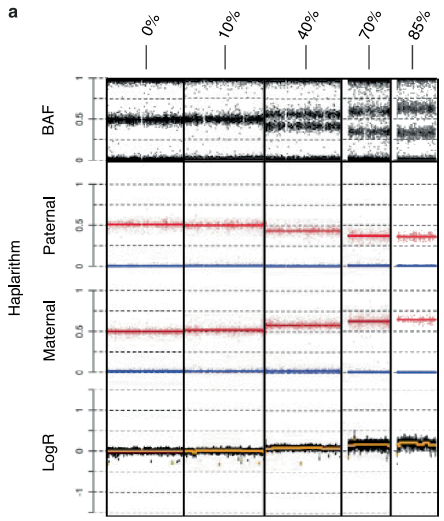


b

| PL number | Group | Tissue | Aberration | Genome coordinates | Length | SNP probes |
|---|---|---|---|---|---|---|
| PL1618 | SPL | EM | Duplication | Chr5:38166170-40845121 | 2678951 | 399 |
| | | CV | Duplication | Chr5:38265653-40851369 | 2585716 | 370 |
| PL245 | SPL | EM | Deletion | Chr5:58814-16708741 | 16649927 | 2918 |
| | | CV | Deletion | Chr5:58814-16708741 | 16649927 | 2918 |
| | | EM | Duplication | Chr7:58814-43206934 | 43148120 | 7187 |
| | | CV | Duplication | Chr7:58814-43216201 | 432010387 | 7190 |
| PL2019 | SPL | EM | Deletion | Chr1:204215542-248928328 | 44712786 | 7353 |
| | | CV | Deletion | Chr1:204219033- 248928328 | 44709295 | 7351 |
| | | EM | Duplication | Chr4:58814-18387778 | 18328964 | 3274 |
| | | CV | Duplication | Chr4:58814-18443081 | 18384267 | 3278 |

**Extended Data Fig. 1 | Mosaicism of > 10% and CNVs > 100 kb are detected by genome haplarithmisis. a**, Different mosaicism degrees for chromosomal trisomy of paternal origin of several PLs. **b**, Detected CNVs for 3 PLs including genome coordinates, length, and number of SNP probes.

https://doi.org/10.1038/s41591-023-02645-5

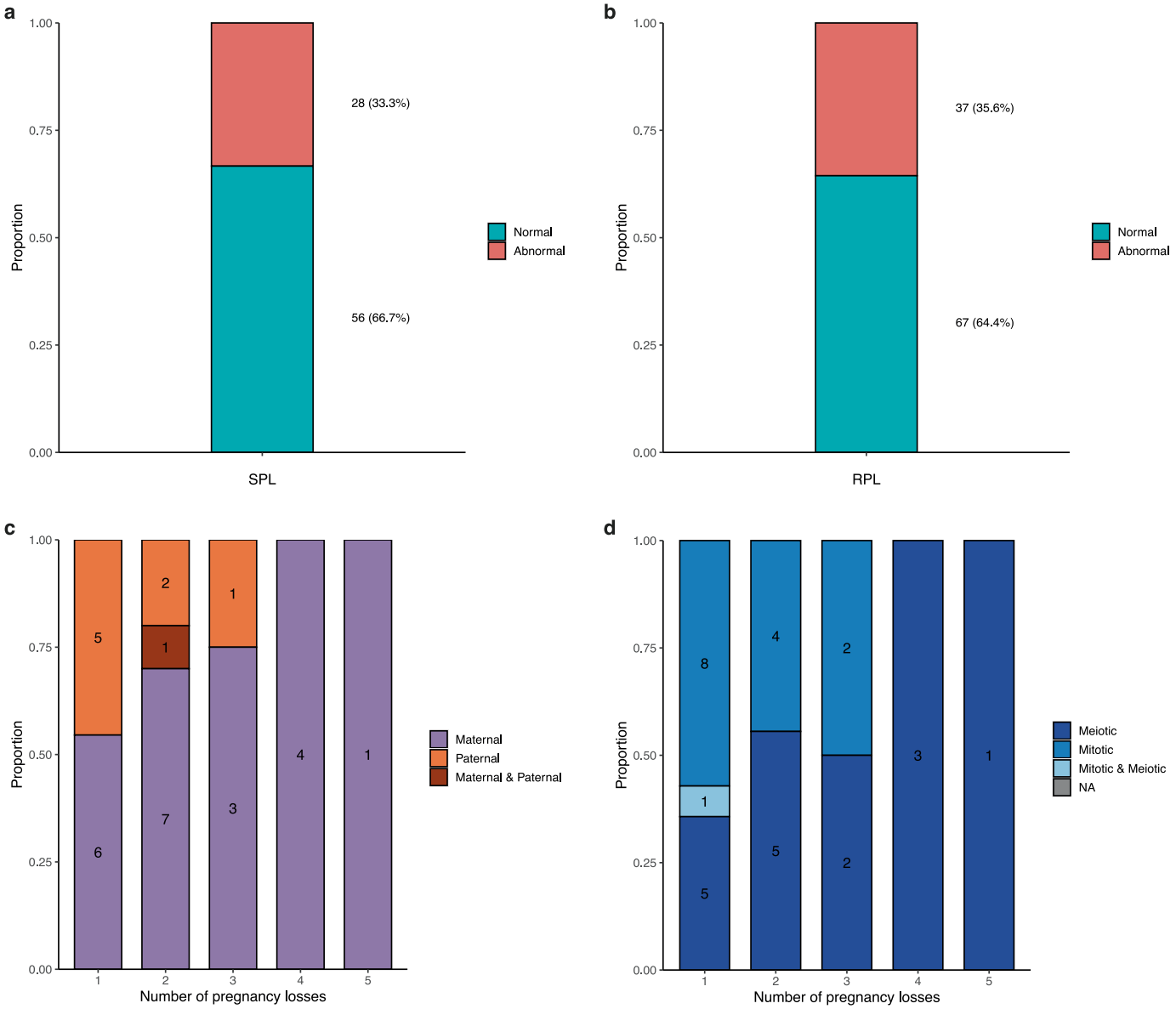


**Extended Data Fig. 2 | Abnormality rate per tissue between SPL and RPL with parental and segregational origin. a**, Abnormality rate of SPL DNA samples (n = 84). **b**, Abnormality rate of RPL DNA samples (n = 104). **c**, Parental origin and number of PLs per family (n = 30). **d**, Segregational origin and number of PLs per family (n = 32).

https://doi.org/10.1038/s41591-023-02645-5

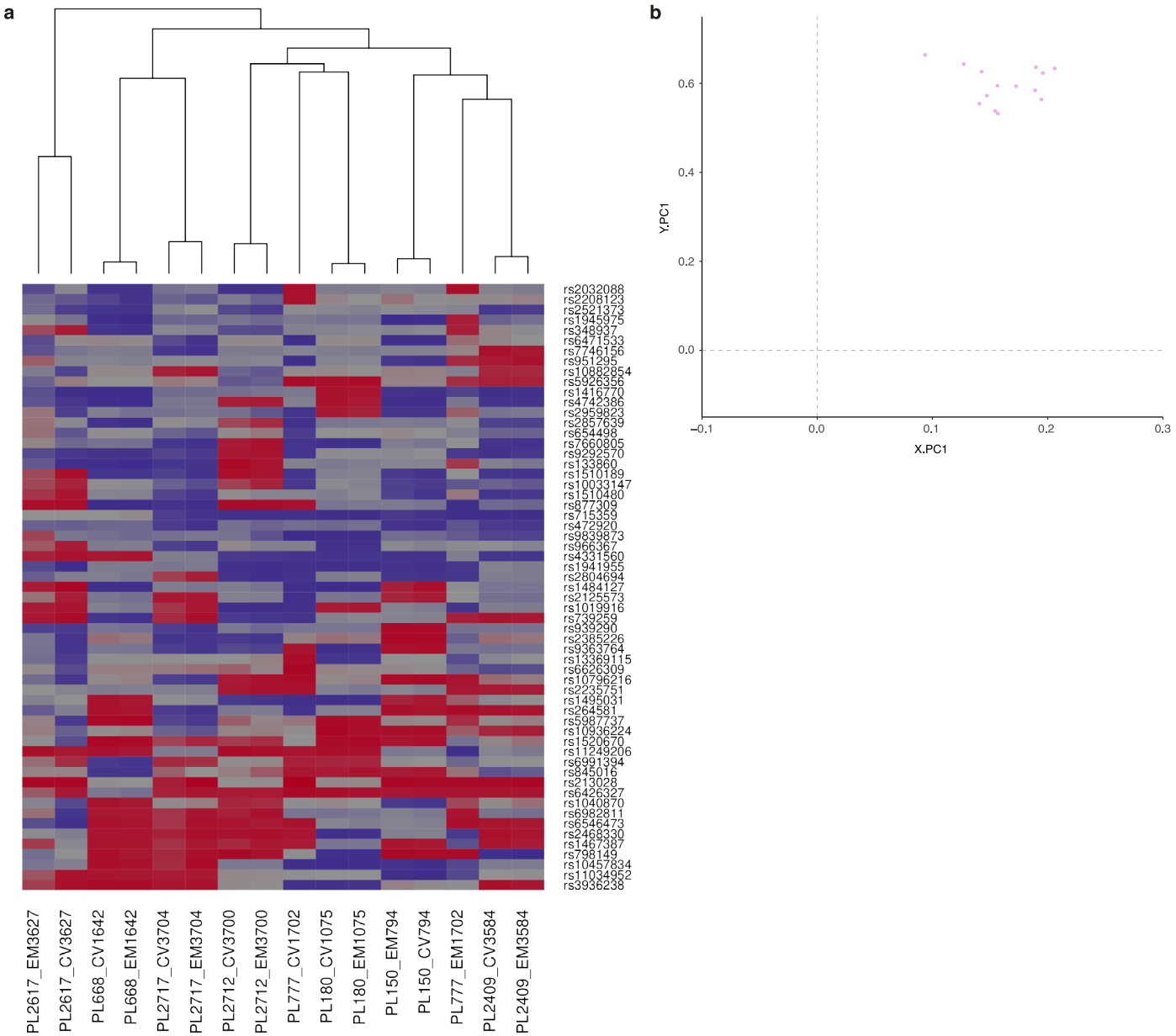


**Extended Data Fig. 3 | Heatmap and PCA of EM and CV tissue samples.** **a**, Heatmap of EPIC array SNP probes (n = 59) of all paired EM and CV tissue samples (n = 13). Hierarchical clustering of the samples was constructed using Euclidian distance and complete linkage and is shown as a dendrogram. **b**, Scatter plot showing the projection of all EM and CV tissue samples (n = 13) into the principal component space generated using reference data for sex prediction (not shown). All chosen samples were female according to the haplotyping analysis and the methylation sex prediction. Grey dashed lines separate the quadrants where male (XY) samples are expected to map to the lower left quadrant and female (XX) samples to the upper right quadrant.

https://doi.org/10.1038/s41591-023-02645-5

a

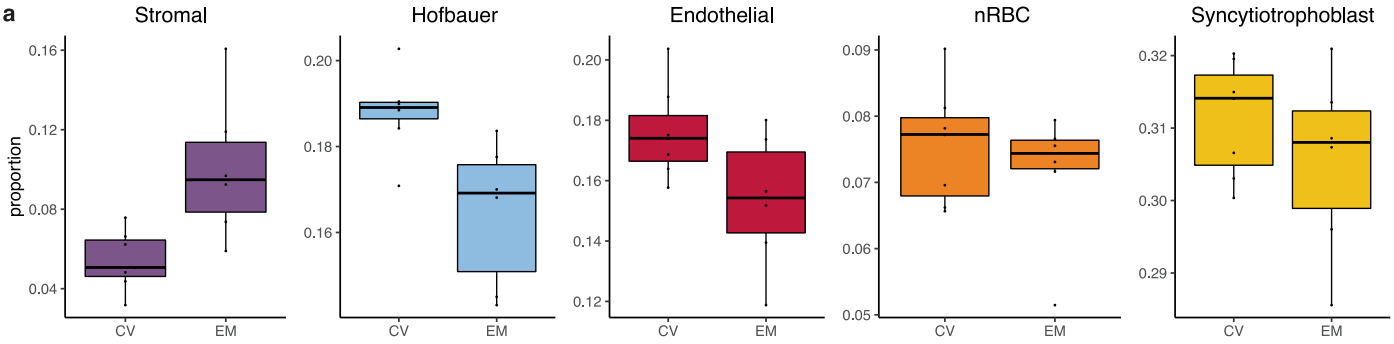


b

| Cell type | Mean (CV) | Mean (EM) | Welch's t-test p-value |
|---|---|---|---|
| Stromal | 0.054 | *0.100* | ***0.024*** |
| Hofbauer | 0.188 | *0.165* | ***0.018*** |
| Endothelial | 0.176 | *0.154* | *0.070* |
| nRBC | 0.076 | 0.071 | 0.451 |
| Syncytiotrophoblast | 0.311 | 0.305 | 0.350 |

**Extended Data Fig. 4 | Predicted cell composition of EM and CV samples based on methylation data. a**, Boxplots showing the predicted cellular composition of the high DNA quality EM (n = 6) and CV (n = 7) samples for each cell type: stromal cells, Hofbauer cells, Endothelial cells, nucleated red blood cells (nRBCs) and syncytiotrophoblast cells. The horizontal lines of the of the boxplot represent the 25$^{th}$ percentile, median and 75$^{th}$ percentile respectively while the whiskers extend to the farthest data point that is no more than 1.5 times the interquartile range (IQR) from the upper or lower quartile. The dots represent individual samples. **b**, Table with mean values of each cell type, P values were calculated with two-sided Welch's T-test.

https://doi.org/10.1038/s41591-023-02645-5

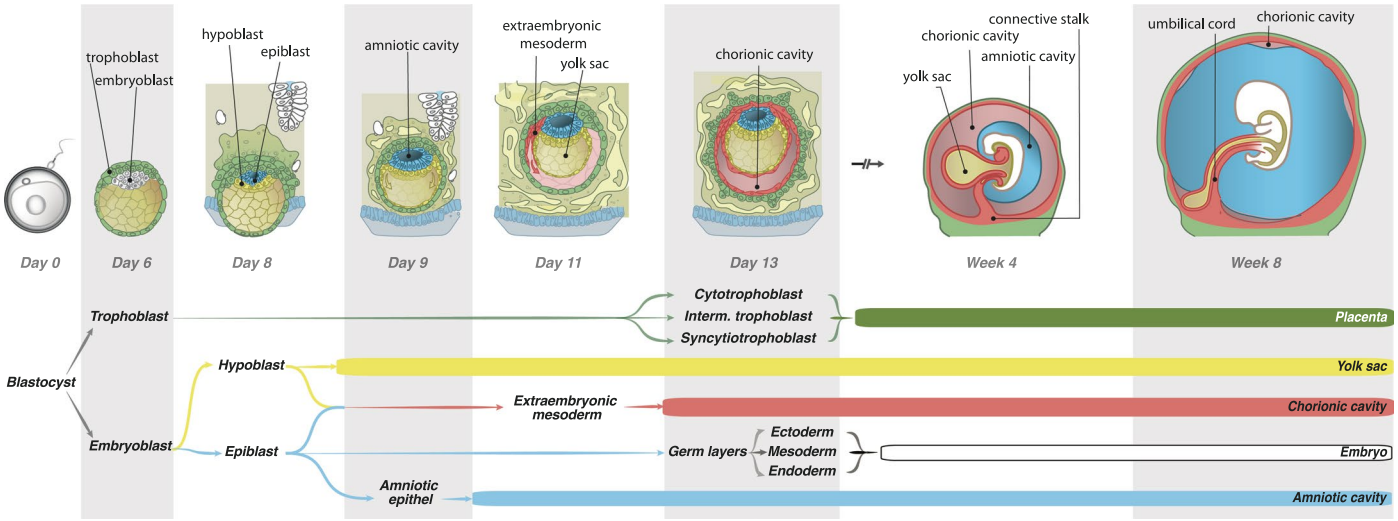


**Extended Data Fig. 5 | Detailed schematic representation of early embryonic development.** Trophoblast and embryoblast lineages develop at day 6, hypoblast and epiblast develop from the embryoblast at day 8, hypoblast develops into the yolk sac, while epiblast develops into the different embryonic germ layers and the embryo and into the amnionic cavity. Extraembryonic mesoderm develops around day 11 from the hypo- and epiblast. The trophoblast cells become the placenta including cytotrophoblast, intermediate trophoblast, and syncytiotrophoblast cells, chorionic villi develop around day 13 from the trophoblast lineage (see also Fig. 2a).

https://doi.org/10.1038/s41591-023-02645-5

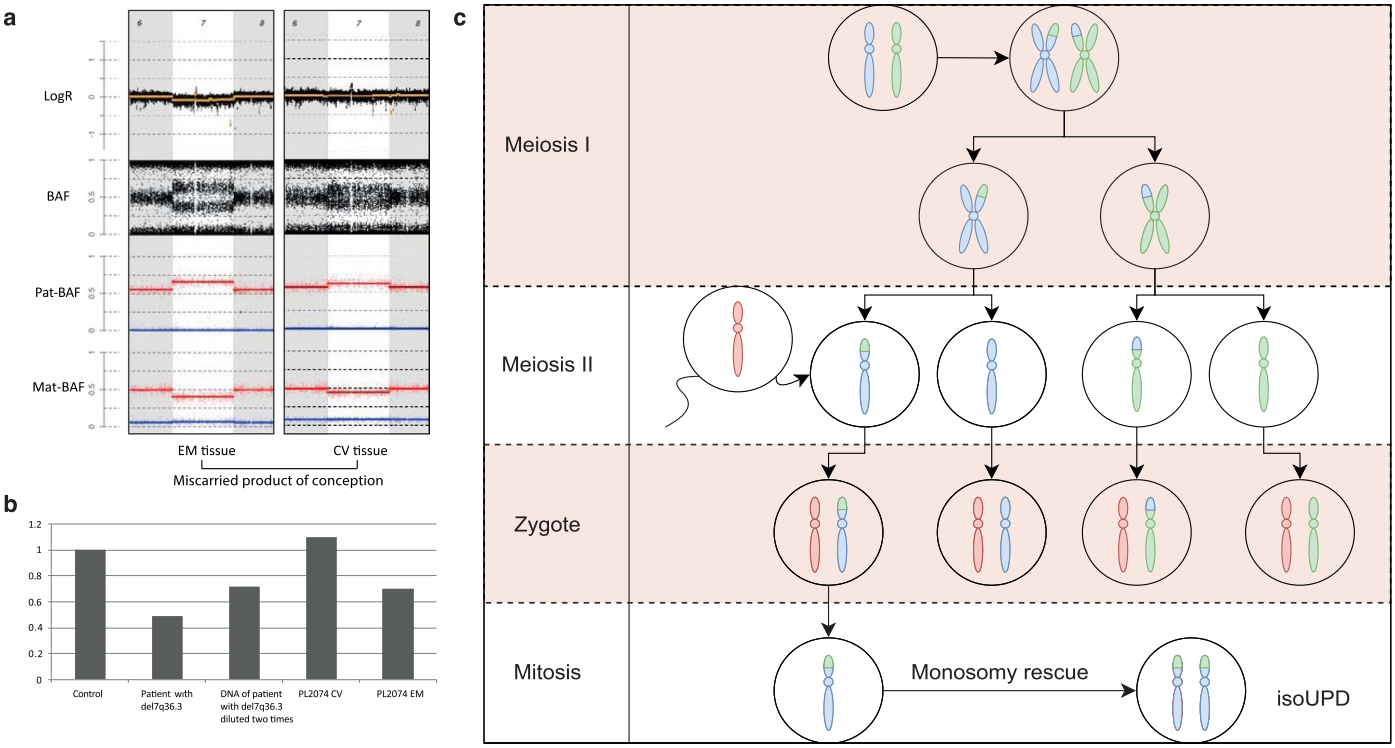


**Extended Data Fig. 6 | Validation of chromosome 7 copy number in PL2074.** **a**, Haplarithm of EM and CV tissue of PL2074, EM shows a 50% mosaic monosomy 7 while CV shows a ~ 30% UPD (copy-neutral) with contamination of maternal tissue. **b**, RT-qPCR results with a diploid control, patient with a 7q36.3 deletion and two times diluted, PL2074 CV (UPD, copy neutral), and PL2074 ( ~ 50% mosaic monosomy 7) with contamination of maternal tissue. **c**, Schematic representation of proposed monosmy-rescue mechanism leading to uniparental disomy (UPD).

https://doi.org/10.1038/s41591-023-02645-5

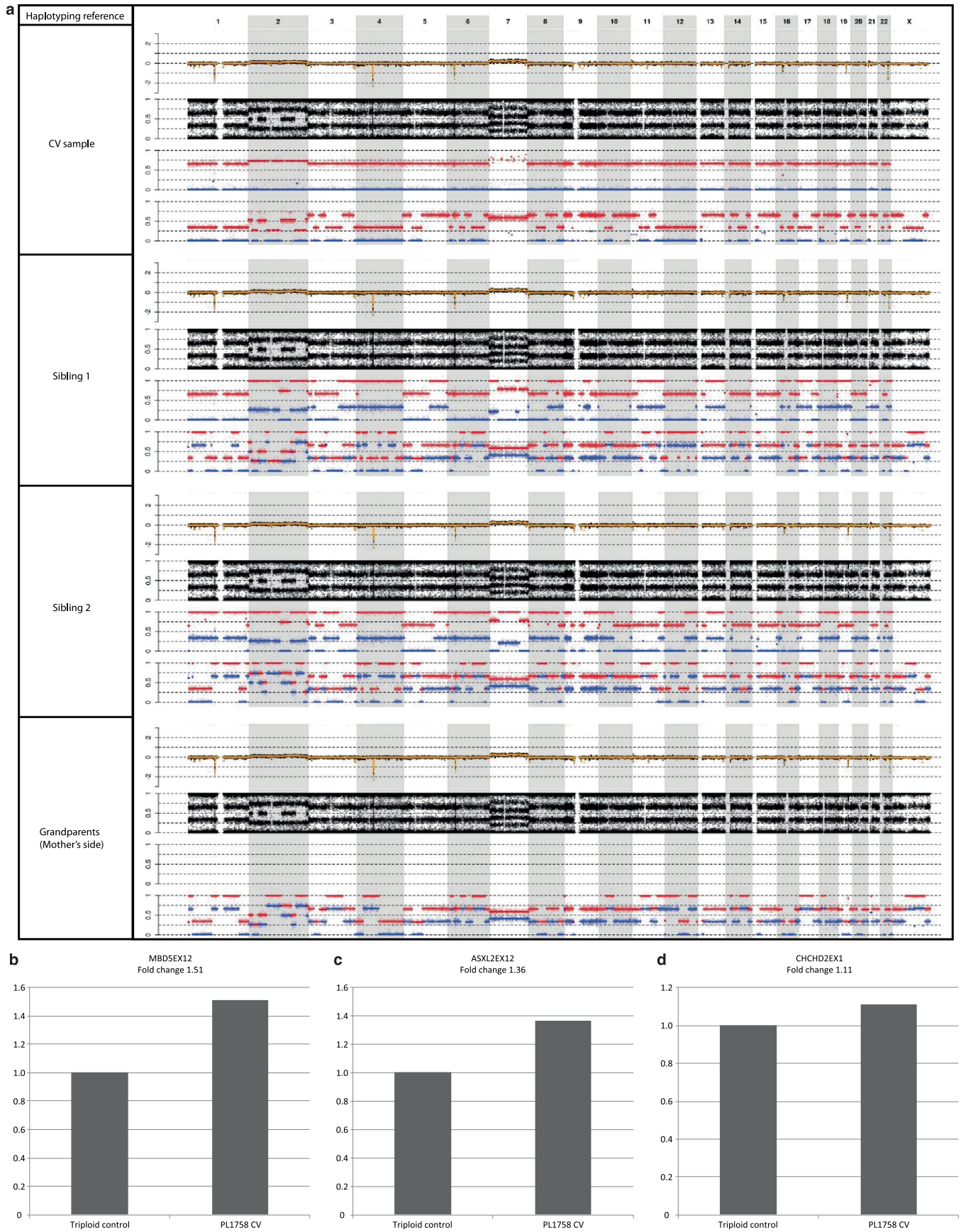


**Extended Data Fig. 7 | See next page for caption.**

https://doi.org/10.1038/s41591-023-02645-5

**Extended Data Fig. 7 | Validation of segregational origin of aberrations in PL1758 CV DNA sample. a**, Haplarithms of fetal EM of PL1758, produced with different references for phasing, namely CV of the same fetus, 2 different siblings, and maternal grandparents. PL1758 shows complex abnormalities with genome-wide triploidy of maternal error origin, and mosaic tetrasomy of Chr 2 and Chr 7, segregational origin appear to be mitotic (Chrs 1, 4, 12), or meiotic II (Chrs 3, 5, 6, 8, 9, 10, 11, 13, 14, 15, 16, 17, 18, 19, 20, 21, 22). Haplarithmisis can accurately determine segregational origin with CV as reference compared to siblings or grandparents as a reference. Validation of PL1758 by RT-qPCR using DNA from spontaneous PL with 69,XXX karyotype and primers for **b**, exon 12 of the *MBD5* gene (2q23.1), **c**, exon 12 of the *ASXL2* gene (2p23.3), and **d**, exon 1 of the *CHCHD2* gene (7p11.2) were used to confirm tetrasomy for Chr 2 and Chr 7 in DNA from CV of PL1758.

nature portfolio

Corresponding author(s): Masoud Zamani Esteki

Last updated by author(s): 25-05-2023

# Reporting Summary

Nature Portfolio wishes to improve the reproducibility of the work that we publish. This form provides structure for consistency and transparency in reporting. For further information on Nature Portfolio policies, see our Editorial Policies and the Editorial Policy Checklist.

## Statistics

For all statistical analyses, confirm that the following items are present in the figure legend, table legend, main text, or Methods section.

| n/a | Confirmed |
|---|---|
| ☐ | ☒ The exact sample size (*n*) for each experimental group/condition, given as a discrete number and unit of measurement |
| ☐ | ☒ A statement on whether measurements were taken from distinct samples or whether the same sample was measured repeatedly |
| ☐ | ☒ The statistical test(s) used AND whether they are one- or two-sided<br>*Only common tests should be described solely by name; describe more complex techniques in the Methods section.* |
| ☐ | ☒ A description of all covariates tested |
| ☐ | ☒ A description of any assumptions or corrections, such as tests of normality and adjustment for multiple comparisons |
| ☐ | ☒ A full description of the statistical parameters including central tendency (e.g. means) or other basic estimates (e.g. regression coefficient) AND variation (e.g. standard deviation) or associated estimates of uncertainty (e.g. confidence intervals) |
| ☒ | ☐ For null hypothesis testing, the test statistic (e.g. *F*, *t*, *r*) with confidence intervals, effect sizes, degrees of freedom and *P* value noted<br>*Give P values as exact values whenever suitable.* |
| ☒ | ☐ For Bayesian analysis, information on the choice of priors and Markov chain Monte Carlo settings |
| ☒ | ☐ For hierarchical and complex designs, identification of the appropriate level for tests and full reporting of outcomes |
| ☒ | ☐ Estimates of effect sizes (e.g. Cohen's *d*, Pearson's *r*), indicating how they were calculated |

*Our web collection on statistics for biologists contains articles on many of the points above.*

## Software and code

Policy information about availability of computer code

| | |
|---|---|
| Data collection | New data was generated for this study. Genome-wide single nucleotide polymorphism profiles in DNAs from maternal and paternal blood, and extraembryonic mesoderm and chorionic villi from the miscarried product of conception of 111 families (114 POCs). SNP genotyping was performed on genomic DNA isolates using Illumina InfiniumTM Global-Screening Array-24 v2.0 and v3.0 BeadChip Kit (Illumina, no. GEO: GLP28939), which contains approximately 665.000 SNP markers with a mean probe spacing of ~4.4 kb and a median probe spacing of ~2.3 kb. Illumina genotyping was performed at the Core Facility of Genomics, Institute of Genomics, University of Tartu, Estonia. |
| Data analysis | All code will be made available on Github. Genotype calls, SNP B-allele frequency values and logR values of all samples were computed using Illumina GenomeStudio 2.0 software. Haplarithmisis was used to compute parental haplarithms. Raw logR-values were smoothed by using a moving average window of five consecutive SNP probes, wave-corrected for GC% bias by a Lowess fit and normalized to a trimmed mean of normal diploid chromosomes. Normalized logR-values were segmented by piecewise-constant fitting (gamma = 14). Levels of mosaicism were calculated based on BAF values or paternal, maternal haplarithm values.<br>Statistical analysis was performed using RStudio version 2023.03.0+386. |

For manuscripts utilizing custom algorithms or software that are central to the research but not yet described in published literature, software must be made available to editors and reviewers. We strongly encourage code deposition in a community repository (e.g. GitHub). See the Nature Portfolio guidelines for submitting code & software for further information.

## Data

Policy information about availability of data

All manuscripts must include a data availability statement. This statement should provide the following information, where applicable:

- Accession codes, unique identifiers, or web links for publicly available datasets
- A description of any restrictions on data availability
- For clinical datasets or third party data, please ensure that the statement adheres to our policy

All SNP array data is available on NCBI Gene Expression Omnibus (GEO; http://www.ncbi.nlm.nih.gov/geo/) accession number GEO: GSE228151. Link for access by the reviewers only: https://www.ncbi.nlm.nih.gov/geo/query/acc.cgi?acc=GSE228151 with token number "gfgjigsylrclrst"

## Human research participants

Policy information about studies involving human research participants and Sex and Gender in Research.

| | |
|---|---|
| Reporting on sex and gender | In our retrospective analysis, sex of the miscarried POC DNA was determined by XX/XY SNP genotyping coverage, visualized in haplarithmisis-produced plots. Sex of the couples was obtained from the "Biobank of populations of Northern Eurasia", Research Institute of Medical Genetics, Tomsk National Research Medical Center (https://ckp-rf.ru/catalog/ckp/507500/). The association between abnormality rate in miscarried POCs and paternal and/or maternal age was investigated. In literature, both paternal and maternal age are shown to have an individual effect on the abnormality rate of miscarried POCs. |
| Population characteristics | In total, 111 couples participated in this study. Age and sex were used in determining the association with abnormality rate in miscarried POCs (see above). Couples (91 families, 94 POCs after exclusion) were divided into sporadic pregnancy loss (42 families and POCs), defined as 1 loss, and recurrent pregnancy loss (49 families and 52 POCs), defined as more or equal to 2 pregnancy losses. |
| Recruitment | The ultrasonography features of early pregnancy loss considered in this study were no cardiac activity or empty gestational sac with a diameter ≥ 25 mm, crown-rump lengths (CRL) ≥ 7 mm for embryos with no cardiac activity, the absence of an embryo and its cardiac activity 14 days after the detection of a gestational sac without a yolk sac, and the absence of an embryo and its cardiac activity 11 days after the detection of a gestational sac with a yolk sac.<br>The most frequent clinical forms of early pregnancy loss were missed abortions followed by anembryonic pregnancies and spontaneous abortions. After ultrasonography diagnosis, women were admitted to gynecological clinics for curettage or medication abortion. Extraembryonic tissues or fragmented gestational sacs were collected in sterile saline and immediately transferred to the Laboratory of Cytogenetics, Research Institute of Medical Genetics, Tomsk National Research Medical Center (Tomsk, Russia) for cytogenetic analysis and cryopreservation. |
| Ethics oversight | Embryonic tissues and parental blood samples were obtained from the "Biobank of populations of Northern Eurasia", Research Institute of Medical Genetics, Tomsk National Research Medical Center (https://ckp-rf.ru/catalog/ckp/507500/). All couples signed an appropriate informed consent for the transfer of their samples to the biobank for scientific research. This study was approved by the local Ethics Committee of the Research Institute of Medical Genetics, Tomsk National Research Medical Center of the Russian Academy of Sciences (Protocol #10, February 15, 2021). Permission was given for the retrospective analysis of the anonymized biological samples of the biobank. |

Note that full information on the approval of the study protocol must also be provided in the manuscript.

# Field-specific reporting

Please select the one below that is the best fit for your research. If you are not sure, read the appropriate sections before making your selection.

☒ Life sciences ☐ Behavioural & social sciences ☐ Ecological, evolutionary & environmental sciences

For a reference copy of the document with all sections, see nature.com/documents/nr-reporting-summary-flat.pdf

# Life sciences study design

All studies must disclose on these points even when the disclosure is negative.

| | |
|---|---|
| Sample size | To calculate the required sample size for the Wilcoxon signed-rank test for matched pairs to test the difference in mosaicism between EM and CV , we assumed a normal parent distribution, a mean percentage of 43% mosaicism in the CV group, a standard deviation (SD) of 30 in both groups, and a correlation between the groups of 0.5. A total sample size of 35 participants was required to test a 15% difference between the EM and CV group, performing a two-sided test using an alpha of 0.05 and a power (1-β) of 0.80. The sample size calculation was performed using G*power 3.1.9.7. |
| Data exclusions | 20 couples have been excluded from data analysis. For proper haplotyping of miscarried POC samples, adequate quality DNA is necessary from the parents as well as POC tissue. For 16 cases there was inadequate quality of DNA for at least one of the required samples. 4 couples were excluded due to one or both parental DNA samples having no parental match with the fetal tissues (not biological parents). |

| | |
|---|---|
| Replication | For 33 DNA samples, DNA quality was insufficient for proper haplotyping. For these samples, DNA was re-isolated and genotyped for analysis. |
| Randomization | The study participants were couples affected by pregnancy loss. From 1745 spontaneous pregnancy loss cases that were karyotyped, 111 families were randomly selected based on the following inclusion criteria: a normal karyotype, availability of parental blood samples and extraembryonic mesoderm and chorionic villi from the miscarried POC, and no identified genetic predisposition for pregnancy loss in the couple. For 91 families (94 POCs), a division was made between sporadic pregnancy loss (42 families and POCs), defined as 1 loss, and recurrent pregnancy loss (49 families and 52 POCs), defined as more or equal to 2 pregnancy losses. |
| Blinding | Prior to data analyses fetal and parental samples were anonymized. The investigators were blinded to group allocation during data collection. |

# Reporting for specific materials, systems and methods

We require information from authors about some types of materials, experimental systems and methods used in many studies. Here, indicate whether each material, system or method listed is relevant to your study. If you are not sure if a list item applies to your research, read the appropriate section before selecting a response.

## Materials & experimental systems

| n/a | Involved in the study |
|---|---|
| ☒ | ☐ Antibodies |
| ☒ | ☐ Eukaryotic cell lines |
| ☒ | ☐ Palaeontology and archaeology |
| ☒ | ☐ Animals and other organisms |
| ☒ | ☐ Clinical data |
| ☒ | ☐ Dual use research of concern |

## Methods

| n/a | Involved in the study |
|---|---|
| ☒ | ☐ ChIP-seq |
| ☒ | ☐ Flow cytometry |
| ☒ | ☐ MRI-based neuroimaging |